Interpretation of Magnetotelluric Results Using Laboratory Measurements

Anne Pommier

Abstract Magnetotelluric (MT) surveying is a remote sensing technique of the crust and mantle based on electrical conductivity that provides constraints to our knowledge of the structure and composition of the Earth's interior. This paper presents a review of electrical measurements in the laboratory applied to the understanding of MT profiles. In particular, the purpose of such a review is to make the laboratory technique accessible to geophysicists by pointing out the main caveats regarding a careful use of laboratory data to interpret electromagnetic profiles. First, this paper addresses the main issues of cross-spatial-scale comparisons. For brevity, these issues are restricted to reproducing in the laboratory the texture, structure of the sample as well as conditions prevailing in the Earth's interior (pressure, temperature, redox conditions, time). Second, some critical scientific questions that have motivated laboratory-based interpretation of electromagnetic profiles are presented. This section will focus on the characterization of the presence and distribution of hydrogen in the Earth's crust and mantle, the investigation of electrical anisotropy in the asthenosphere and the interpretation of highly conductive field anomalies. In a last section, the current and future challenges to improve quantitative interpretation of MT profiles are discussed. These challenges correspond to technical improvements in the laboratory and the field as well as the integration of other disciplines, such as petrology, rheology and seismology.

Keywords Electrical conductivity · Impedance spectroscopy · Electromagnetics · Magnetotellurics

1 Introduction

By probing the electrical structure of the Earth, magnetotelluric (MT) surveys represent one of the most important and valuable tools to image the Earth's crust and mantle and

A. Pommier (✉)
School of Earth and Space Exploration, Arizona State University,
Tempe, AZ, USA
e-mail: apommier@asu.edu

infer rock properties. Because electrical conductivity is a transport property that can be measured at both laboratory (millimeters) and field (kilometers) scales, the richness of the MT technique is enhanced because we have a large database of electrical conductivity measurements in the laboratory that critically contribute to help the interpretation of MT profiles. Laboratory measurements of electrical conductivity of geomaterials (melts, minerals, fluids) have reached a point where interesting, intriguing and provocative interpretations of electromagnetic data in terms of composition, temperature and geological processes (such as subducted fluids or mantle plume detection) are possible and needed.

This paper attempts to provide an overview of cross-spatial-scale comparisons between electrical data from laboratory experiments and MT results from the field. Due to space limitations, it is unfeasible to review exhaustively all the literature that interprets MT results using laboratory measurements. Therefore, the issues and challenges covered in this article are focused in a particular direction: making laboratory techniques accessible to geophysicists, with the aim of pointing out the main caveats regarding a careful use of laboratory data as part of the interpretation of MT profiles. This is in part motivated by the recent rapid expansion of other geophysical experiments, for example, EarthScope US-Array seismic network, which enables more detailed seismic models and interpretations relevant to the electrical work. The reader is referred to other recent reviews for specific topics that are not considered in detail in the present paper: Evans (2012) for the review of the conductivity structure in the continental and oceanic crust and mantle; Yang (2011) for a review of electrical anomalies in the continental crust; Tyburczy and Fisler (1995), Nover (2005), Tyburczy (2007) and Yoshino (2010) for comprehensive reviews of the conductivity of minerals and conduction mechanisms attributed to different types of charge carriers (ions, electrons, defects and vacancies); and Guéguen and Palciauskas (1994) for mixing rules for multi-phase materials.

This review paper will first focus on the most important aspects of cross-spatial-scale comparisons between field and laboratory electrical data. Impedance spectroscopy (laboratory technique) and MTs (field technique) are both used to investigate conduction mechanisms, and it is quite remarkable to see how well laboratory results agree with conductivity models of the mantle derived from MT data (Fig. 1). However, as detailed in the following section of this paper, cross-spacial-scale comparisons are not straightforward (e.g., Duba 1976, 1982; Sato and Ida 1984; Bahr 1997) and a major point that has been widely discussed regards the relevance of laboratory measurements, taken on small samples and usually at high frequencies, to MT data that probe (and average over) length and depth scales of tens to hundreds of kilometers at lower frequencies. Laboratory measurements on small samples or compacted powders may partly miss natural textural complexity that must be taken into account in the final interpretation. On the other hand, the significance of the information that can be extracted from laboratory results may also be easily underestimated or used incorrectly. Besides issues related to scaling effects (i.e., scaling laboratory measurements to physical scales of field measurements), the use of electrical data on melts and rocks to interpret MT profiles implies that laboratory measurements are taken at conditions representative of those prevailing in the Earth's interior. Improvements in difficult experimental setups are more than ever a topical issue. Recent technical efforts in the laboratory have made it possible to perform high-quality and in situ electrical measurements with improved control of pressure, temperature, redox conditions, thermodynamic conditions, sample composition (including fluid content) and texture (e.g., Huang et al. 2005; Caricchi et al. 2011; Yang and McCammon 2012; Yoshino et al. 2012).

The second part of this paper will present an overview of some of the critical scientific questions for which a laboratory-based interpretation of MT data has significantly
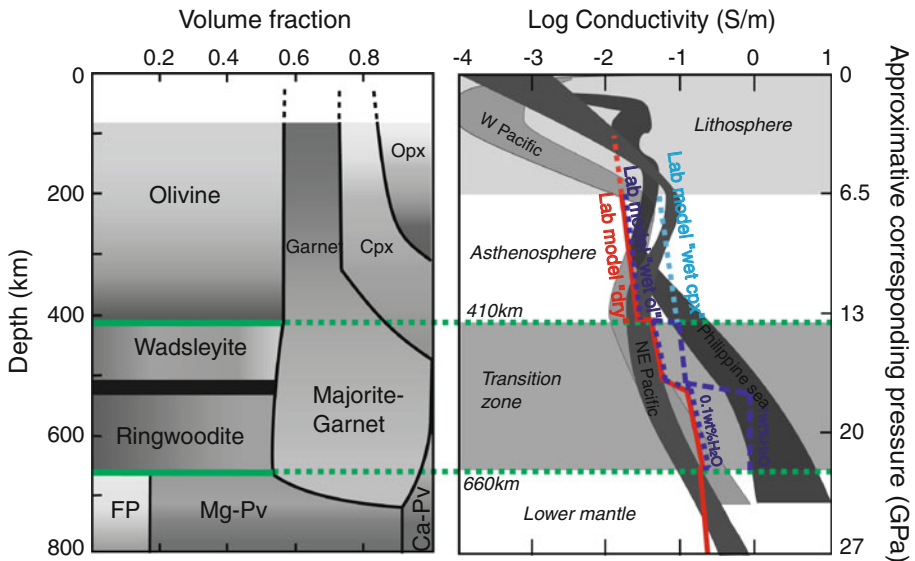
Fig. 1 Depth–conductivity profiles: comparison between laboratory and field data. Laboratory profiles calculated using SIGMELTS (*right*), based on a defined mineralogical composition (*left*, redrawn from Stachel et al. 2005, *FP* ferropericlase, *Pv* perovskite) and using a mantle adiabat with a potential temperature of 1,300 °C. Dry (*red*) and wet (*blue*) scenarios considered. Because of a limited electrical database for the lower mantle, it is assumed that conductivity lower mantle = conductivity perovskite. Field data are from Lizarralde et al. (1995) (NE Pacific), Baba et al. (2010) (W Pacific and Philippine sea)

improved our understanding of the Earth's interior and stimulated the scientific community over the past years. Among these questions is the quest to document and characterize the role of "water" in the Earth's mantle. These investigations have benefited not only from improvements in field and laboratory electromagnetic techniques (e.g., Simpson and Bahr 2005), but also from laboratory hydrogen solubility and diffusion studies (e.g., Mackwell and Kohlstedt 1990; Demouchy and Mackwell 2003, 2006; Du Frane and Tyburczy 2012) that significantly contributed to understanding the speciation and behavior of water in minerals and melts. Impedance measurements on hydrous geomaterials (e.g., Gaillard 2004; Wang et al. 2006; Pommier et al. 2008; Manthilake et al. 2009; Poe et al. 2010; Ni et al. 2011a; Yang et al. 2011) have quantified the increase in conductivity due to the presence of water and have led to the elaboration of conductivity models of hydrous minerals and melts (e.g., Pommier and LeTrong 2011; Yoshino and Katsura 2012). The conflicting conclusions between some laboratory results (Wang et al. 2006; Yoshino et al. 2006), in particular regarding hydrous olivine, demonstrate the difficulty of these measurements as well as the need for further investigations. These models at least agree on the fact that certain very conductive field anomalies detected in some regions at particular depths of the upper mantle (e.g., Lizarralde et al. 1995; Baba et al. 2006) cannot solely be attributed to the presence of dissolved water, thereby stimulating further electrical studies on other materials such as hydrous melt. Other scientific questions that will be considered regard the hypothesis of carbonatites to explain very high conductivities (Gaillard et al. 2008; Yoshino et al. 2010, 2012) and the investigation of electrical intrinsic and extrinsic anisotropies in mantle minerals (e.g., Yoshino et al. 2006; Dai and Karato 2009a; Poe et al. 2010; Yang 2012).

Future challenges to improve the quantitative interpretation of MT data will be discussed in the last section of this paper. The need for high quality of laboratory and field data is obviously critical to any quantitative interpretation of MT results. Regarding electrical field studies, the acquisition of high-quality data at very long periods as well as the resolution of conductivity models based on data inversion represents some of the challenges currently faced by the MT community to improve the technique. Nevertheless, the most interesting challenge possibly concerns the integration of other disciplines as part of the quantitative interpretation of electrical data. Petrological and geochemical knowledge is required to constrain the composition, temperature and pressure at which laboratory data should be used to interpret electric profiles. Promisingly, some studies have also superimposed seismic results and MT profiles in order to constrain better the field structure (e.g., Key and Constable 2002; Chen et al. 2009). Analyzed together with—and not subordinated to—seismic surveys, electrical investigations significantly further our understanding of mantle heterogeneities (thermal, chemical, textural). Another important step toward a complete interpretation of electromagnetic data is the integration of magma chamber dynamics as part of the interpretation of MT profiles in volcanic regions. Newly developed empirical relationships between conductivity and viscosity of naturally occurring silicate melts can lead to new understanding in such areas. The quantitative interpretation of MT data is emerging as a powerful tool in the variety of disciplines that probe Earth materials at crust/mantle depths (petrology, mineral physics, seismology, numerical geodynamics, tectonics), and the coming years promise significant new contributions to our understanding of the Earth's interior.

2 Cross-Spatial-Scale Comparisons: A View from the Laboratory

2.1 Principle of Electrical Measurements in the Laboratory and in the Field

At the scale of the laboratory (millimeters), conductivity experiments consist of the measurement of the electrical complex impedance[1] (e.g., Huebner and Dillenburg 1995). Impedance represents the total opposition to a current flux in response to an AC signal (e.g., Roberts and Tyburczy 1994). Being a complex number, it can be expressed as a magnitude and a phase, or a real and an imaginary part, or equivalently a resistance and a capacitance. From complex impedance (Z^*) data, the complex conductivity σ^* of a sample is obtained by multiplying Z^* by a geometric factor[2] and can be written as (e.g., Roberts and Tyburczy 1994):

$$\sigma^* = \sigma + j\omega\varepsilon' \tag{1}$$

σ being the real conductivity (S/m), ω the angular frequency (Hz) and ε' is the real part of the permittivity (F/m) ($j^2 = -1$). Practically, what is measured in the laboratory is the electrical resistance R (ohm), from which σ is then obtained (using the geometric factor).

$$\sigma = 1/(G \cdot R) \tag{2}$$

The temperature and pressure dependence of the conductivity of melts and minerals follows an Arrhenian formalism (e.g., Tyburczy and Fisler 1995):

---

[1] It is worth noticing that methods other than impedance spectroscopy have been proposed (e.g., Volarovich and Tolstoi 1936; Bockris et al. 1952; Volarovich et al. 1962), but they do not account for the frequency dependence of electrical conductivity and will not be considered in this paper.

[2] The geometric factor accounts for the sample dimensions. For instance, for a cylindrical geometry with current circulating radially inside the cylinder, $G = (2\pi L)/[\ln(d_e/d_i)]$ with L the cylinder length and d_e and d_i the outer and inner diameters, respectively (e.g., Gaillard 2004).

$$\sigma = \sigma_0 \cdot \exp[-(Ea + P\Delta V)/RT] \qquad (3)$$

with σ_0 the pre-exponential term (S/m), Ea the activation energy (J/mol), P the pressure (Pa), ΔV the activation volume (cc/mol), R the universal gas constant (8.3143 J mol^{-1} K^{-1}) and T the temperature (K). In a plot Re(Z^*) versus Im(Z^*), the resistance R corresponds to the intersection of the sample response to a scan in frequency f (usually from MHz to mHz) with the real axis (e.g., Huebner and Dillenburg 1995). For a defined temperature and pressure, this value will not depend on the frequency (contrary to the dielectric permittivity which is frequency dependent). By discriminating between the different polarization effects using a scan in frequency, the impedance technique allows a careful investigation of conduction processes at high temperature in solids (de Bruin and Franklin 1981). The determination of R from an impedance spectrum provides the sample's electrical conductivity, and the rest of the spectrum (at frequencies higher than the one of the intersection with the real axis) expresses the frequency dependence of the sample and in particular its dielectric permittivity, providing critical information regarding the different conduction and relaxation mechanisms (e.g., Roberts and Tyburczy 1991; Moynihan 1998). The information about high-frequency mechanisms is not directly useful as part of MT data interpretation since field measurements consider lower frequencies (longer periods, $>10^3$ s) (e.g., Roberts and Tyburczy 1991, 1999). The reader is referred to studies by Bauerle (1969), Simonnet et al. (2003) and Pommier et al. (2010a) for technical details about impedance measurements and to the works by Roberts and Tyburczy (1994), Huebner and Dillenburg (1995), Roling (1999) and Yoshino and Katsura (2012) for details about the interpretation of impedance spectra for geological materials.

In the field, MT surveys measure a broad spectrum of natural geomagnetic fluctuations as a power source for electromagnetic induction (Simpson and Bahr 2005) over a chosen electromagnetic sounding period ($=1/f$) range. The period is directly related to the penetration depth of the electromagnetic field and to the Earth's conductivity structure. From these fluctuations measured at the surface, the variation in the electrical field within the Earth's interior is obtained as a function of the period and is then expressed as a function of depth and dimensions. A last step of data processing converts electrical field variations into electrical resistivity ρ ($=1/\sigma$) variations. As impedance measurements, MT measurements are used to probe conduction (or semiconduction) mechanisms that control the capability of a material to carry an electrical current (e.g., Chap. 8 in Simpson and Bahr 2005). And as the laboratory community, the MT community also considers electrical conductivity as a real number, assuming that, at low frequency, there is no imaginary component in the response of the material. Details about data analysis and modeling can be found in Simpson and Bahr (2005), Chave and Jones (2012).

2.2 Laboratory–Field Data Comparison: Simple Approach and "Forward" Modeling

There are two main approaches to interpret field electrical data using laboratory results. First, laboratory data can be simply "superimposed" to MT profiles, as shown in Fig. 1. In this case, the conductivity structure is constrained by actual observations of MT responses over a range in frequency and for different locations. Electrical conductivity as a function of depth is calculated through the inversion of MT data and compared to laboratory-based models (e.g., Xu et al. 1998; Khan et al. 2011). One example is shown in Fig. 2a. In their study, Xu et al. (1998) defined a laboratory-based conductivity-depth model for the upper mantle and compared it to MT results from the literature in order to investigate the composition of the Earth's mantle. This simple approach has been (and still is) widely used
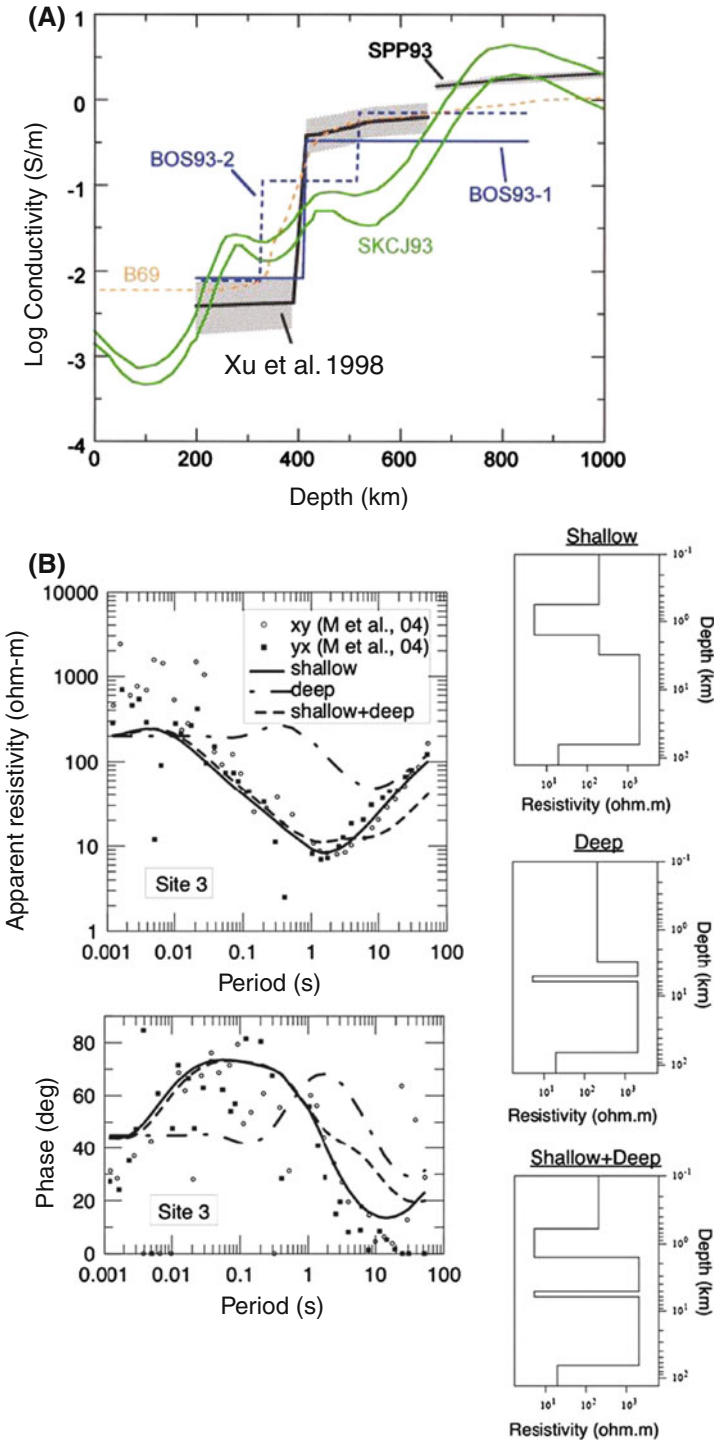
◀ **Fig. 2** Different approaches for cross-spatial-scale comparisons. **a** "Simple" comparison with superimposition of laboratory-based model to MT profile (Xu et al. 1998). Laboratory results are in *black*. Field data from Banks (1969) (B69), Bahr et al. (1993) (BOS93), Schultz (1990) and Kurtz et al. (1993) (SKCJ93) and Shankland et al. (1993) (SPPP93). **b** Forward modeling of the conductivity of Mount Vesuvius (Pommier et al. 2010c). 1D simulations of the effect of a shallow and deep conductor (resistivity–depth structures on the *right*) on the transfer functions (*left*). Predicted MT responses based on a petro-physical model are compared to the field data from Manzella et al. (2004) (M et al. 04) for their Site 3 on Mount Vesuvius

and is particularly convenient since it represents the simplest and quickest way to compare field and laboratory data, with the aim of placing compositional constraints. However, this approach does not require accounting for the geological context, and it does not provide constraints on the dimensions of a field anomaly.

The second approach consists of forward calculations that predict the MT responses over a frequency range (usually ~ 10 to $>10^4$ s) and at arbitrary geographic locations based on a hypothetical model of the conductivity structure (e.g., Xu et al. 2000; Dobson and Brodholt 2000; Toffelmier and Tyburczy 2007; Pommier et al. 2010c). These studies used electrical laboratory measurements of minerals and melts as part of forward calculations for mantle P and T conditions and compared them to field data. This approach promotes the use of thermodynamic and petrological knowledge that would not be necessarily resolved by the MT data inversion process, since these pieces of information can be integrated from the beginning of the modeling to the hypothetical structure. The example presented in Fig. 2b concerns Mount Vesuvius volcanic area, Italy (Pommier et al. 2010c). In this study, the initial structure was based on petrological knowledge of the area, previous geophysical constraints and geochemical observations. Based on a petro-physical conductivity model, the forward approach allowed the test of hypotheses regarding the dimensions and storage conditions of two conductive bodies (shallow brine and magma reservoir), the predicted MT responses being each time compared to the existing MT dataset for Mount Vesuvius. This approach contributed to placing important constraints on the brine (~ 0.5 km depth, 1.2 km thick, 5 ohm-m resistive), which is the most conductive body below the volcano. Our forward model also suggested that the present-day reservoir at 8 km depth probably has a resistivity >100 ohm-m, which is best interpreted by two possible scenarios: (1) a low-temperature and crystal-rich deep magma reservoir or (2) a hotter magma (tephriphonolitic melt at 1,000 °C containing 3.5 wt% H_2O and 30 vol.% crystals) interconnected in the more resistive solid carbonates (45 % melt, 55 % carbonates).

We can also underline a third kind of modeling, close to a forward approach and which consists of a direct inversion of field data for a defined composition and temperature (e.g., Khan et al. 2006a; Verhoeven et al. 2009; Khan and Shankland 2012).

The following subsections will focus on some critical points regarding cross-spatial-scale comparisons. In particular, the issue of reproducing in the laboratory the conditions that prevail in the Earth's crust and mantle will be detailed.

2.3 Reproducing Sample's Structural and Textural Parameters in the Laboratory

One of the biggest challenges in reproducing field conditions in the laboratory regards the structure and texture of geomaterials. The inhomogeneity of rocks over long length scales (hundreds of meters to kilometers) probed by field studies is hardly reproducible in the small-size samples (a few millimeters) for laboratory measurements. Measurements on drill core samples involve sample sizes much bigger than the ones for high-pressure

measurements (up to ~ 1 m^3 vs. a few mm^3), and therefore, one may think that they would be more relevant for a comparison with field data. As noticed by Bahr (1997), the bulk resistivity in the study on drill core samples by Rauen and Lastovickova (1995) differs at 500 °C by a factor 3, 10 and 20 for basalt, gabbro and granite samples, respectively. The important variations in conductivity that have been observed between different drill core rocks for a same temperature and pressure (e.g., Kariya and Shankland 1983; Rauen and Lastovickova 1995) are much too large to be explained by compositional effects (expected to be $\sim$ less than a factor 2) and can probably be attributed to differences in the abundance, size and distribution of cracks in the rock samples (Bahr 1997). In fact, electrical measurements on drill core rocks require considering and controlling numerous parameters that affect the electrical measurements, including the number and geometry of cracks, the effect of fluids possibly present in the cracks, the variations in grain size, the foliation of the rock (e.g., Stesky 1986). By their size (typically 2–5 mm), high-pressure samples are generally homogeneous compared to the field, enabling an easier discrimination of the effect of every controlled parameter (chemical composition, anisotropy) on their bulk conductivity. However, when compared to field data, experiments on homogeneous samples require accounting for the effect of structural settings on large-scale field conductivities (particularly in tectonic contexts where abundant fluid-filled cracks in rocks are expected), which is still poorly constrained.

The problem of reproducing and controlling connectivity and permeability of different phases (solid or fluid) highlights the need for new experiments and mixing models. Characterizing bulk conductivity as a function of interconnectivity is critical since a conductive solid or liquid phase must be interconnected over kilometers, that is, on a scale measurable by MTs, to explain field anomalies. Among the attempts that have been made, Bahr (1997) proposed a conductivity model that combines the effective-medium theory (EMT) with the percolation theory. Guéguen et al. (1997) also revisited the EMT models in order to improve the characterization of porosity and permeability. In the case of partially molten materials, the effect of melt geometry on electrical conductivity has been pointed out by several studies such as Sato and Ida (1984), Glover et al. (2000), Roberts and Tyburczy (2000), ten Grotenhuis et al. (2005), Yoshino et al. (2010) and Caricchi et al. (2011). In texturally equilibrated partially molten materials, melt geometry is controlled by its composition, the surrounding matrix and interfacial energies, the latter being usually characterized by the determination of the melt fraction and dihedral angles (Fig. 3, von Bargen and Waff 1986; Watson and Brennan 1987). Interconnected melt topologies occur
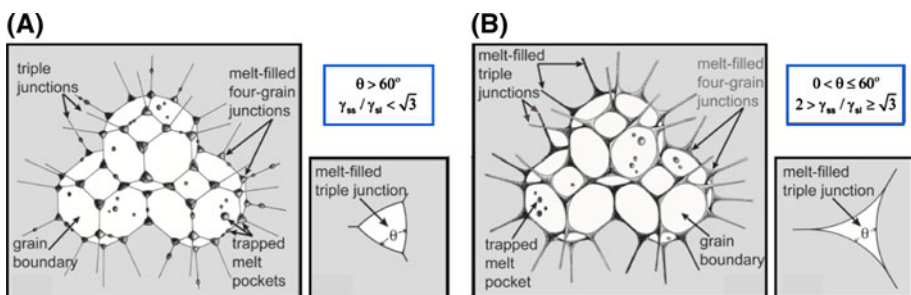

Fig. 3 Geometry of grain boundaries and dihedral angles (from Kohlstedt and Mackwell 2010). **a** Isolated melt pockets and **b** interconnected melt channels along grain edges. *S* solid (grain), *L* liquid (melt), θ dihedral angle, γ surface tension. The melt phase controls the bulk conductivity if interconnected ($\theta < 60°$) within the solid matrix

for values of dihedral angle less than 60°. The importance of dihedral angles has also been highlighted by seismic studies (e.g., Takei 2000; Hier-Majumder and Courtier 2011). In natural systems, melt geometry is also influenced by other parameters such as anisotropy of surrounding crystals (Faul et al. 1994). However, conductivity models accounting for these parameters are lacking in the current literature. Most commonly used solid–fluid mixing models for electrical conductivity are summarized in Table 1 after Glover et al. (2000) and ten Grotenhuis et al. (2005).

Details about grain boundary transport can be found in Roberts and Tyburczy (1993). Only a few studies focused on the effect of grain boundary composition and, in particular, the effect of conductive grain boundary phases on the bulk conductivity (Ducea and Park 2000; Watson et al. 2010). For instance, sulfide in grain boundaries enhances the bulk conductivity of polycrystalline olivine, and the effect of adding a significant amount of sulfide (1 vol.%) is similar to the effect of adding 0.01–0.1 % hydrogen to olivine (Watson et al. 2010). In the field, melt-related sulfides (e.g., Evans et al. 2011) have been suggested to explain conductivities. Graphite in grain boundaries has also been suggested as a bulk conductivity enhancer (Duba and Shankland 1982; Frost et al. 1989), but this has not been tested by thorough electrical conductivity studies in the laboratory. Moreover, the fields of stability of graphite and sulfide do not cover the entire depth range of the upper mantle (e.g., Frost and McCammon 2008), implying to be careful with applications to the field.

2.4 Control of Pressure (Depth) and Temperature in the Laboratory Experiments

Experiments in the laboratory have to be conducted at relevant pressure and temperature for the Earth's interior in order to be compared to field data. This requires use of appropriate setups and conductivity cells, which can turn out to be a real challenge, in particular regarding the minimization of thermal gradients at high pressure (Hernlund et al. 2006). Also, placing two to four electrodes across a sample that is compressed and heated presents several engineering and technical challenges. Different electrical cells adapted to specific pressure ranges are presented in Fig. 4. The different materials and the sample dimensions are chosen to minimize thermal and pressure gradients as well as chemical interactions with the sample. Constraints on pressure estimates are based on previous calibration experiments using phase transition of minerals, such as the quartz–coesite transition occurring at 3.1 GPa and 1,000 °C (Bohlen and Boettcher 1982) or the fayalite–spinel transition at 5.75 GPa and 1,200 °C (Yagi et al. 1987). Usually, the accuracy of the pressure reading is about ±0.3 GPa using a high-pressure device (K. Leinenweber, personal communication). Recent development in high-pressure techniques can allow more accurate pressure determination using pressure marker (e.g., MgO, Au) by means of synchrotron X-ray radiation [see Ohta et al. (2008) for electrical conductivity measurements of lower-mantle minerals in diamond anvil cell (DAC) and Yoshino et al. (2011) for measurements in the multi-anvil, with pressure being determined by volume change in the pressure marker].

Because of the high dependence of conductivity to temperature, minimization of the temperature gradient across the assembly (and, in particular, across the zone where the sample is placed) is critical. Thermal gradient can be estimated using several thermocouples along the assembly or by conducting experiments of mineral phase transitions (high-pressure setups). A common method is the two-pyroxene thermometry experiment performed by Lindsley and Dixon (1976) on the pressure range 5–35 kbar. This experiment is based on the T-dependent phase transition between enstatite and diopside at a defined pressure and consists of measuring the composition of pyroxene in different spots of the

Table 1 Currently used mixing rules for conductivity calculations (σ_{eff} is the effective bulk conductivity, X_i is the volume fraction of phase i, s stands for solid and m for melt), after Glover et al. 2000 and ten Grotenhuis et al. 2005. Note that two-phase mixing equations can be combined to model the bulk conductivity of 3 or more phases (e.g. Ducea and Park 2000 who used the HS-model for the bulk conductivity of a fluid-solid assemblage, the conductivity of the fluid (melt + sulphide) being calculated using the cube model)

Name	Equation	Phases (min; max)	Description	References
Parallel model	$\sigma_{\text{eff}} = \sum_{i=1}^{n} X_i \sigma_i$	(1; many)	Parallel i layers with conductivity arranged axially to current flow	For example Guéguen and Palciauskas (1994)
Perpendicular model	$\dfrac{1}{\sigma_{\text{eff}}} = \sum_{i=1}^{n} \dfrac{X_i}{\sigma_i}$	(1; many)	Parallel i layers with conductivity arranged normally to current flow	For example Guéguen and Palciauskas (1994)
Random model	$\sigma_{\text{eff}} = \prod_{i=1}^{n} \sigma_i^{X_i}$	(1; many)	Arbitrary shaped and oriented i volumes distributed randomly	Shankland and Waff (1977)
Effective-medium theory	$\sum_{i=1}^{n} X_i \left[\dfrac{\sigma_i - \sigma_{\text{eff}}}{\sigma_i + 2\sigma_{\text{eff}}} \right] = 0$	(1; many)	Media with located spherical i inclusions	Berryman (1995), Khan and Shankland (2012)
Hashin–Shtrikman upper bound (HS+)	$\sigma_{\text{eff}+} = \sigma_m + \dfrac{1-X_m}{\frac{1}{\sigma_s - \sigma_m} + \frac{X_m}{3\sigma_m}}$	(2; 2)	Derived from effective-medium considerations (spheres model, melt interconnected)	Hashin and Shtrikmann (1962)
Hashin–Shtrikman lower bound (HS−)	$\sigma_{\text{eff}-} = \sigma_s + \dfrac{X_m}{\frac{1}{\sigma_m - \sigma_s} + \frac{1-X_m}{3\sigma_s}}$	(2; 2)	Derived from effective-medium considerations (spheres model, melt in isolated pockets)	Hashin and Shtrikmann (1962)
Cube model	$\sigma_{\text{eff}} = \sigma_m \left[1 - (1 - X_m)^{\frac{2}{3}} \right]$	(2; 2)	Cubic grains surrounded by a layer (melt) of uniform thickness	Waff (1974)
Tubes model	$\sigma_{\text{eff}} = \frac{1}{3} X_m \sigma_m + \sigma_s (1 - X_m)$	(2; 2)	Equally spaced tubes (melt) in a rectangular network (triple junctions)	Grant and West (1965)
Modified Archie's law	$\sigma_{\text{eff}} = \sigma_s (1 - X_m)^p + X_m^n \sigma_m$ where $p = \dfrac{\log(1-X_m^n)}{\log(1-X_m)}$, and n is a constant	(1; 2)	Derived from the conventional Archie's law (e.g., Watanabe and Kurita 1993) by considering boundary conditions implied by geometrical constraints	Glover et al. (2000)

capsule: The ratio of the two phases corresponds to a defined temperature. Temperature gradient across the sample is of several °C and depends on the cell assembly (Hernlund et al. 2006). Information about reproducibility of high-pressure experiments (multi-anvil) can be found in Leinenweber et al. (2012).

2.5 Control of Time and Redox Conditions in Experiments

As previously pointed out by Duba (1976), time and redox conditions (usually described by the oxygen fugacity, noted fO_2) are probably not important variables for electrical conductivity at the mantle scale (time is sufficient for most chemical reactions to reach equilibrium, and fO_2 is controlled by the mineralogical assemblage) but are critical at the scale of the laboratory, because buffering a sample at a defined fO_2 is experimentally challenging and the usually short duration of most experiments does not account for kinetics.

Kinetics of chemical reactions between the sample and the surrounding parts of the conductivity cell can be fast enough to affect the measurement at the timescale of the experiment (e.g., Pommier et al. 2010b). This requires choosing carefully the parts of the conductivity cell in order to minimize chemical interactions with the sample. For example, at most relevant P and T conditions for the Earth's interior, graphite (commonly used in furnaces for high-pressure experiments) reacts with iron (Fe_2O_3) in the melt (Holloway et al. 1992). This loss of iron from the melt influences the sample bulk conductivity and therefore may affect the measurement.

Hydrous samples are particularly sensitive to the effect of experimental duration on their electrical properties. Water diffusivity within minerals and melts is very high ($\sim 10^{-10}$ m^2/s at 1,000 °C for hydrogen diffusion in silicate minerals (Kohlstedt and Mackwell 1998, 1999) and $\sim 10^{-9}$–10^{-11} m^2/s at 1,000 °C for water diffusion in silicate melts (Baker et al. 2005 and references therein)); therefore, it is common to observe a significant water loss from hydrous samples after a run whose duration would have given time for dissolved water to migrate out of the sample (e.g., Satherley and Smedley 1985). Hence, it is necessary to carefully check the water content of a hydrous sample both before and after the experiment. In polycrystalline materials, the presence of a fluid phase will control the bulk conductivity if interconnected between the small grains of laboratory samples. Therefore, the longer the run duration at high temperature ($> \sim 800°C$), the higher is the risk of dehydrating the grains and forming an interconnected fluid layer between the grains (see discussion in Yoshino et al. 2009). If these processes are not carefully observed and documented, the electrical results will be inappropriate to apply to field data. Actually, on a geological timescale and for coarse-grained rocks, diffusion experiments show that hydrogen transport by bulk mineral diffusion will be limited due to the large grain size of mantle rocks (e.g., Demouchy 2010a, b).

The time effect is complicated regarding measurements on partially molten materials, and the change in conductivity across the temperature interval of crystallization can have different explanations. First, the timescale of the experiment can be faster than the time needed for liquid and crystals to reach chemical equilibrium. This may significantly affect bulk conductivity of partial melt since it has been shown to depend strongly on melt's chemical composition (e.g., Roberts and Tyburczy 1999; Gaillard and Iacono Marziano 2005). Second, as demonstrated by Piwinskii and Duba (1974) for an albite melt, the observed change in melt conductivity across the interval of crystallization is not necessarily related to melting as previously suggested by Khitarov and Slutskii (1965), but can be explained by kinetics of order–disorder at the atomic scale if not enough time is allowed for the melt to order when it is heated to subsolidus temperatures (Duba et al. 1976) (Fig. 5).
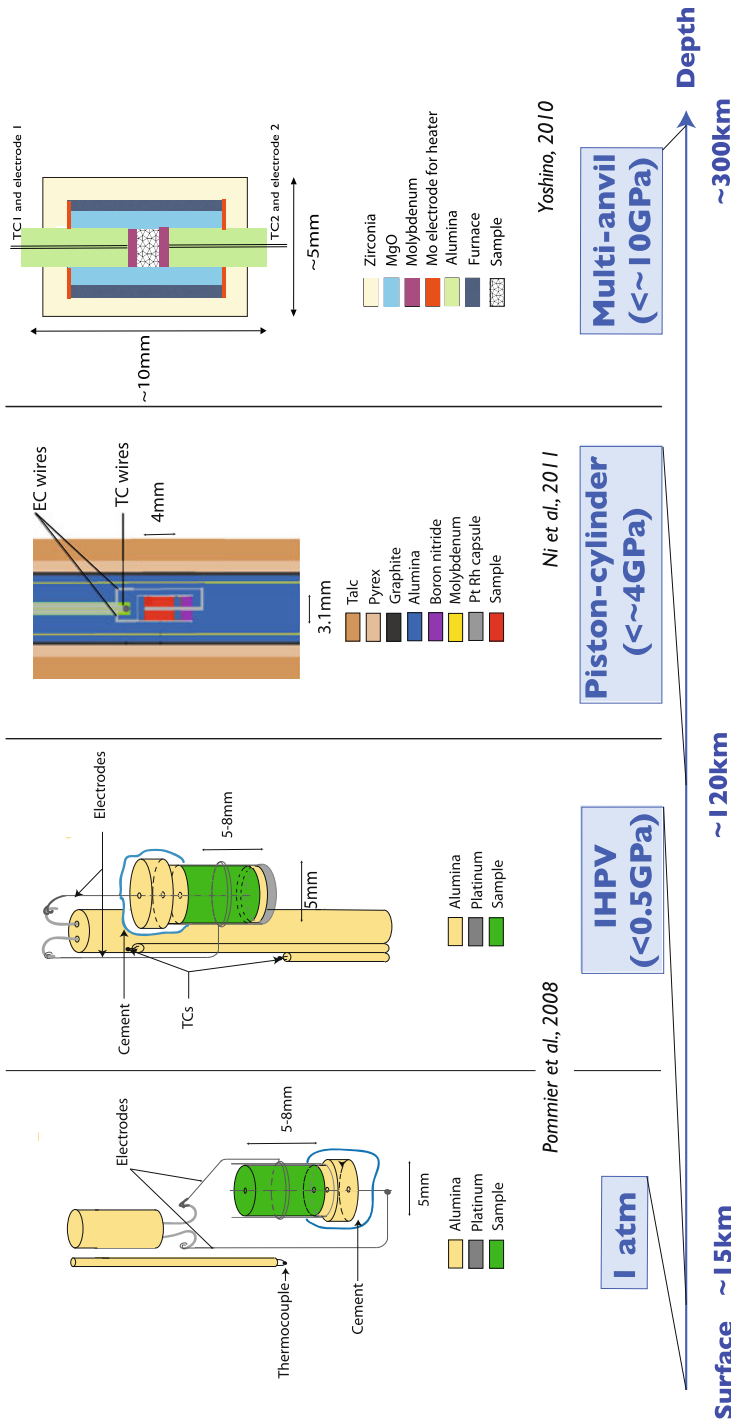
Fig. 4 Example of two-electrode conductivity cells with sample dimensions for different pressure ranges of investigation, with corresponding depths in the Earth. The choice of the materials aims to minimize thermal and pressure gradients inside the sample. *IHPV* internally heated pressure vessel. More details about each cell can be found in the cited references. For measurements in piston cylinder, see also Yang et al. (2011), and in multi-anvil, Xu et al. (1998) and Dai and Karato (2009a, b, c)

Fig. 5 Electrical conductivity of albite (after Duba et al. 1976). Colored area corresponds to the interval of crystallization. Red and blue lines are measurements from Khitarov and Slutskii (1965) upon heating and cooling cycles. *Vertical* intervals show the conductivity change at defined *T* measured by Piwinskii and Duba (1974). Albite melt was heated for 526 h at 1,080 °C, then for 1,199 h at 1,100 °C and then for 1,486 h at 1,111 °C. Duba and coworkers deduced that after 3,200 h at *T* > 1,080 °C, albite melt is not completely disordered and that the conductivity change measured by Khitarov and Slutskii was not (only) due to the effect of melting. This study shows that the measured bulk conductivity upon heating (*red line*) is not an equilibrium value
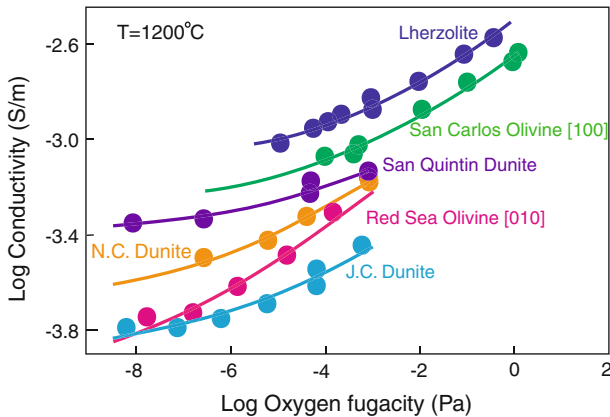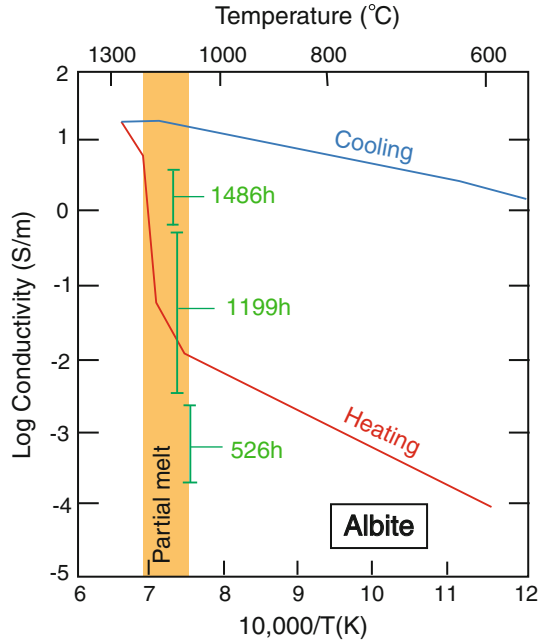
Fig. 6 The effect of oxygen fugacity on the conductivity of mantle materials (after Duba and Constable 1993). All the data are fitted by the following model: $\sigma = \sigma_0 + \sigma_1 (fO_2)^{0.182}$ with σ_0 and σ_1 being variables

It is also important to note that experimental duration can affect the textural equilibration of partial melts, which can consequently modify the conductive paths inside the sample. It has been shown that when stress is removed at the end of a shear deformation experiment, surface tension causes the melt to relax back to a homogeneous distribution over a period of a few hours (Parsons et al. 2008). Therefore, the duration of conductivity experiments on previously deformed partially molten materials must be short enough to maintain the texture of the sample, and the texture evolution must be documented by post-experiment characterization using, for example, scanning electron microscope (SEM) or optical microscopy techniques.

The conductivity of Earth materials can be very sensitive to redox conditions. The effect of oxygen fugacity (fO_2) on silicate melt conductivity is negligible at a first approximation (Waff and Weill 1975; Pommier et al. 2010b), which is not the case for several rocks and minerals, particularly iron-bearing lherzolite and olivine (e.g., Duba and Nicholls 1973; Duba et al. 1974; Sato 1986; Duba and Constable 1993; Constable and Duba 2002; Constable 2006; Dai et al. 2008) (Fig. 6). Therefore, electrical experiments on these minerals have to be performed at controlled redox conditions that are relevant for the conditions of the investigated portion of the Earth's interior. Also, changes in temperature (during heating or cooling) drive changes in oxygen fugacity and thus conductivity (Constable and Duba 2002). Oxygen fugacity can be easily controlled in gas-medium apparatus, particularly 1-atm gas-mixing furnaces, in which fO_2 sensors such as zirconia probes can be installed for real time and in situ fO_2 monitoring. The control of redox conditions is still rather approximate in solid-state transmitting medium of high-pressure apparatus (piston cylinder, multi-anvil). Boron nitride (BN) can be used as part of the cell assembly to apply reduced conditions (Wendlandt et al. 1982). As pointed out by Bagdassarov et al. (2011), molybdenum (Mo) electrodes combined with a BN environment buffer the fO_2 around IW 0.8. Using Mo, rhenium (Re) or BN parts for cell assemblies may affect olivine conductivity by less than 0.1 order of magnitude (Bagdassarov et al. 2011).

3 Quantitative Interpretation of Field Data Motivated by Scientific Questions

Electrically conductive regions of the Earth's interior have been interpreted in terms of hydrous silicate minerals, melt, aqueous fluids or other very conductive phases such as graphite and metallic oxides. The effect of anisotropy of conductive phases has also been suggested to explain enhanced conductivities. The depth of investigation of electromagnetic surveys depends on the motivation: Electromagnetic studies in the near surface have been encouraged as part of oil prospecting, metalliferous mining and geothermal investigation (e.g., Atekwana et al. 2000; Nabighian and Asten 2002; Meju 2002 and references therein; Constable and Srnka 2007), while deeper investigations have aimed to understand volcano feeding systems (Jones and Dumas 1993; Manzella et al. 2004), earthquake zones (Chen et al. 2009), crustal structure (e.g., Jones and Gough 1995; Ogawa et al. 2001; Le Pape et al. 2012) and, more generally, the structure of the Earth's mantle (Lizarralde et al. 1995; Utada et al. 2003; Kelbert et al. 2009).

This section presents different examples of high conductive anomalies for which laboratory measurements have significantly improved our interpretation of MT images. The following examples do not deal with MT studies applied to geothermal investigation and mining exploration.

3.1 The Quest to Document and Characterize Hydrogen ("Water")[3] in the Earth's Crust and Upper Mantle

The Earth's interior is thought to contain a non-negligible amount of hydrogen that was present in the earliest Earth (e.g., Righter and Drake 1999) or that is supplied to the planet

---

[3] As mentioned, for instance, by Karato (2006), it is hydrogen and not molecular water that affects the physical and chemical properties of silicates. However, the term water is also commonly used since the concentration of chemical species is usually measured as wt% of oxide in the geology literature. Meaning for water content unit: In olivine (Fo$_{90}$), 0.1 wt% H_2O corresponds to 1.65×10^4 atoms of H per 10^6 Si.

from its surface through different plate-tectonic processes (e.g., subduction of water-rich pelagic sediments and release of bounded water during mineral breakdown or melting, Ohtani et al. 2004). Although the hypothesis of a "dry" mantle cannot be totally excluded (e.g., Yoshino et al. 2008), a water content of ~0.005–0.02 wt% H_2O in the upper mantle is usually considered, based on measurements of water contents on mid-ocean ridge basalt (MORB) glasses and mantle minerals (Bell and Rossman 1992a; Jambon 1994; Michael 1995; Saal et al. 2002; Peslier 2010). Higher estimates have been suggested for the mantle transition zone 410–660 km deep (with a water storage capacity >0.4 wt% H_2O just above the 410-km discontinuity, Hirschmann et al. 2005). Quantifying the absolute water content in the Earth's mantle, inferring its distribution and flux and understanding its partitioning are important questions because hydration greatly influences the physical properties of the mantle (among them rheology and electrical conductivity) (Mackwell et al. 1985; Inoue et al. 1998; Jacobsen et al. 2004; Huang et al. 2005; Manthilake et al. 2009) and is therefore critical to our understanding of processes on microscopic-to-global scales as well as of the evolution of the planet. Actually, hydrogen is involved in several key geodynamic processes such as slab subduction (e.g., Ohtani et al. 2004), induced melting of the mantle wedge (Gaetani and Grove 2003), the genesis of continental flood basalts and komatiites (e.g., Parman et al. 1997). Direct petrologic measurements of hydrogen content in samples at the surface (e.g., in quenched lava, xenoliths, fluid inclusions) may not be representative of the hydrogen content in the source region (Demouchy and Mackwell 2003, 2006; Peslier and Luhr 2006; Peslier et al. 2008). Therefore, the combination of laboratory studies with geophysical probing (electrical and seismic) of hydrogen reservoirs in the mantle is needed to provide estimates of hydrogen content in the Earth's interior (e.g., Karato 2006). Among the recent attempts to provide estimates of hydrogen content, one can mention Inoue et al. (2010) that proposed, based on hydrogen-partitioning experiments as well as laboratory and field electrical studies, a model of "water" distribution in the Earth's mantle and concluded that the mantle transition zone may be an important hydrogen reservoir, containing up to one-third of the H_2O mass of Earth's oceans. Hydrogen can be stored in minerals, melt or even exist as a free water phase, stimulating challenging laboratory investigations at mantle pressure to interpret electromagnetic anomalies.

3.1.1 Hydrous Olivine and High-Pressure Polymorphs

Olivine and high-pressure polymorphs wadsleyite and ringwoodite[4] are the most abundant minerals in the Earth's upper mantle; therefore, attention has been focused on their capability to store hydrogen (e.g., Smyth 1987; Kohlstedt et al. 1996; Smyth et al. 2003) and on their influence on physical properties, such as viscosity and, in particular, electrical conductivity (e.g., Huang et al. 2005; Wang et al. 2006; Yoshino et al. 2006, 2009; Manthilake et al. 2009; Poe et al. 2010; Yang et al. 2011; Yoshino and Katsura 2012). Differences in conductivity between olivine, wadsleyite and ringwoodite are particularly important as part of comparisons with MT data because conductivity-depth profiles are much better constrained if we know at which depth discontinuities (corresponding to phase transitions) are expected.

The recent blossoming of electrical investigations of hydrous olivine takes its roots in conductivity calculations in the 1990s (Karato 1990; Constable 1993), with conductivity of hydrous olivine being computed based on experimentally determined hydrogen diffusion

---

[4] The transition between olivine and wadsleyite is known as "the 410 km discontinuity," and the transition between wadsleyite and ringwoodite occurs at ~525 km depth (see Fig. 1).

coefficients (Mackwell and Kohlstedt 1990). The proposed model by Karato (1990) esti-
mates the increase in olivine conductivity due to the presence of hydrogen by relating
electrical conductivity to the concentration of the charged species ("hydrogen") and its
diffusion coefficient. As discussed by Karato (2006), this model was used to interpret MT
data before having been tested experimentally (e.g., Lizarralde et al. 1995; Hirth et al.
2000; Simpson 2002; Tarits et al. 2004), and unfortunately, when laboratory experiments
later tested this model (e.g., Huang et al. 2005; Wang et al. 2006), it turned out that its
validity is only partial and that hydrous olivine conductivity is not only dependent on
hydrogen solubility and diffusivity in olivine but also depends on more complicated
mechanisms involving Mg-site vacancies and electron holes (e.g., Yoshino et al. 2009).
This is a clear example of the need for constraints from laboratory experiments as part of
conductivity modeling and MT data interpretation.

Electrical measurements in the laboratory on hydrous olivine and polymorphs at high
pressure and temperature have benefited from recent technical advances in the impedance
technique applied to measurements under pressure.[5] In addition to the study by Romano
et al. (2009), two laboratories have investigated the electrical properties of hydrous
polycrystalline olivine and high-pressure polymorphs, and a summary of the resulting
conductivity models is presented in Table 2. Several charge transport mechanisms con-
trolling the bulk electrical conductivity of hydrous olivine, wadsleyite and ringwoodite at
the atomic scale punctuate the role of proton, small polaron and Mg-site vacancies (e.g.,
Yoshino et al. 2009):

$$\sigma = \sigma_p + \sigma_h + \sigma_v \qquad (4)$$

with σ the bulk conductivity, σ_p the proton conductivity, σ_h the conductivity of small
polaron (hopping of electrons between ferric and ferrous iron sites) and σ_v the conductivity
of vacancies. Note that σ refers to intra-grain conductivity and does not account for the
conductivity attributed to hydrogen in grain boundaries. At high temperature, if dehy-
dration of olivine is significant, the fluid phase along the grain boundary can form a thin
layer that will significantly contribute to the measured conductivity. Recent measurements
on hydrous single crystals (Yoshino et al. 2006; Poe et al. 2010; Yang 2012) will be
discussed in Sect. 3.2 dedicated to anisotropy. The higher conductivity of hydrous wads-
leyite and ringwoodite (compared to hydrous olivine) results from the fact that a higher
amount of hydrogen can be stored in their structure (e.g., Karato 2006) and at high
pressure, thus enhancing conductivity.

The obvious discrepancy between laboratory results (Karato and coworkers finding a
much more important effect of water on olivine conductivity than Yoshino and coworkers
and Poe et al. 2010) (Table 2; Fig. 7) has resulted in an ongoing debate concerning the
explanation of the difference in conductivities (Yoshino et al. 2009; Dai and Karato 2009c;
Yoshino and Katsura 2012). This highlights the challenging aspect of these experiments
and the difficulty to control many critical (and possibly unknown) parameters. Uncer-
tainties arise from how the grain size is characterized and applied to calculate bulk con-
ductivity (Yang and Heidelbach 2012), from the quantification method of the water content
in the sample before and after every experiment and from the technique and protocol used

---

[5] Historically, hydrous olivine has not been the first hydrous phase to be investigated experimentally using
conductivity measurements. First attempts to measure the electrical properties of hydrous geomaterials had
been previously made on a hydrous granitic melt, Lebedev and Khitarov (1964); on granite with a free water
phase, Olhoeft (1981); on a hydrous basaltic melt, Satherley and Smedley (1985). However, because of
several experimental issues, particularly water loss during the experiment, they can hardly be applied to
interpret field data.

Table 2 Conductivity models of hydrous olivine, wadsleyite and ringwoodite (experiments on polycrystalline samples). (C_w is the water content, T is the temperature (K), R is the universal gas constant (J mol⁻¹ K⁻¹)). See text for details. Starting material in the studies by Manthilake et al. 2009 and Yoshino et al. 2008 is natural olivine from China. In all other studies, starting material is natural San Carlos olivine (Arizona)

Conductivity models – Yoshino and coworkers

OLIVINE (Yoshino et al., 2009): $\sigma = \sigma_0^i \exp\left(\frac{-H_i}{RT}\right) + \sigma_0^h \exp\left(\frac{-H_h}{RT}\right) + \sigma_0^p C_w \exp\left(-\frac{H_0 - \alpha C_w^{1/3}}{RT}\right)$

σ_0^i (S/m)	H_i (kJ/mol)	σ_0^h (S/m)	H_h (kJ/mol)	Log σ_0^p	H_0 (kJ/mol)	α
$10^{4.73}$	223	$10^{2.98}$	165	$10^{1.9}$	88.7	0.16

WADSLEYITE (Yoshino and Katsura, 2012): $\sigma = \sigma_0^h \exp\left(\frac{-H_h}{RT}\right) + \sigma_0^p C_w \exp\left(-\frac{H_0 - \alpha C_w^{1/3}}{RT}\right)$

σ_0^h (S/m)	H_h (kJ/mol)	σ_0^p (S/m)	H_0 (kJ/mol)	α
$10^{2.46}$	140	$10^{1.40}$	80.0	0.02

RINGWOODITE (Khan and Shankland, after Yoshino et al., 2008 and Yoshino and Katsura, 2009): $\sigma = \sigma_0^p C_w \exp\left(-\frac{H_0 - \alpha C_w^{1/3}}{RT}\right) + \sigma_0^{Fe} X_{Fe} \exp\left(-\frac{H_0^{Fe} - \alpha^{Fe} X_{Fe}^{1/3}}{RT}\right)$

T (K)	σ_0^p (S/m)	H_0 (kJ/mol)	α	σ_0^{Fe} (S/m)	H_0^{Fe} (kJ/mol)	α^{Fe}
<1000	$10^{1.44}$	108	0.67	$10^{2.67}$	206	2.14
>1000	$10^{1.44}$	108	0.67	$10^{4.0}$	201	1.55

Conductivity models – Karato and coworkers

OLIVINE (Wang et al., 2006): $\sigma = A_1 \exp\left(-\frac{E1+PV1}{RT}\right) + A_2 C_w^r \exp\left(-\frac{E2+PV2}{RT}\right)$

A_1 (S/m)	A_2 (S/m)	r	E1/E2 (kJ/mol)	V1/V2 (cc/mol)
$10^{2.4}$	$10^{3.1}$	0.62	154/87	2.4/-

WADSLEYITE (Huang et al., 2005; Dai and Karato, 2009c): $\sigma = A_1 \exp\left(-\frac{E1+PV1}{RT}\right) + A_2 C_w^r \exp\left(-\frac{E2+PV2}{RT}\right)$

A_1 (S/m)	A_2 (S/m)	r	E1/E2 (kJ/mol)	V1/V2 (cc/mol)
$10^{2.1}$	$10^{2.1}$	0.72	147/88	-/-

RINGWOODITE (Huang et al., 2005): $\sigma = A_1 \exp\left(-\frac{E1+PV1}{RT}\right) + A_2 C_w^r \exp\left(-\frac{E2+PV2}{RT}\right)$

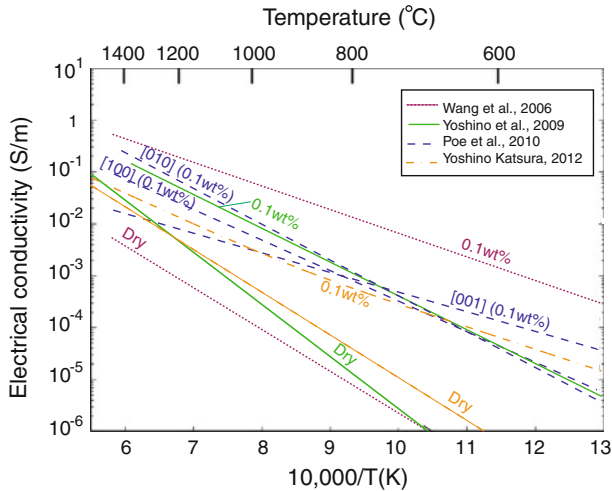| A_1 (S/m)	A_2 (S/m)	r	E1/E2 (kJ/mol)	V1/V2 (cc/mol)
-	$10^{3.6}$	0.69	-/104	-/-

Fig. 7 Electrical conductivity of dry and hydrous olivine (San Carlos) as a function of temperature (after Evans 2012). Data from Wang et al., Yoshino et al. and Yoshino and Katsura are from measurements on polycrystalline olivine samples at 4, 10 and 16 GPa, respectively. Data from Poe et al. are from measurements on single crystal at 8 GPa and are labeled with crystallographic orientation followed by water content (ppm). It is important to note that these models have been extrapolated. To avoid sample dehydration, measurements have been taken at: 600–1,000 °C (Wang et al. 2006), <∼700 °C (Yoshino et al. 2009), <800 °C (Poe et al. 2010). Model by Yoshino and Katsura is based on measurements taken at T up to ∼1,730 °C. Extrapolation at higher T provides a first approximation of the conductivity, but their use as part of MT data interpretation must account for the uncertainty regarding these extrapolated values

to measure the water content. An adequate technique is the one by Bell et al. (2003) and revised by Withers et al. (2012), who determined the absorption coefficients specific for olivine and necessary for water measurements in that mineral by Fourier transform infrared spectroscopy.

Recent studies that aim to integrate these laboratory results as part of conductivity-depth modeling of the Earth's mantle have either proposed separate conductivity models of the mantle for each database (e.g., Khan and Shankland 2012) or made an attempt to reconcile the differences between results. For instance, Jones et al. (2012) proposed a model of conductivity based on statistically derived parameters from existing datasets that satisfy proton conduction equations. The use of the laboratory data as part of conductivity-depth modeling is unquestionably needed as part of cross-spatial-comparisons, but it must be kept in mind that laboratory conductivity equations have been obtained for defined experimental conditions that do not always appear in the final mathematical formalism, although these conditions can influence conductivity. An example is that related to the effect of redox conditions and is provided in Fig. 8. Based on their laboratory conductivity measurements on wadsleyite and ringwoodite, Huang et al. (2005) suggested that the MT soundings below the North Pacific (Utada et al. 2003) are best explained by 0.1–0.2 wt% H_2O in the mantle transition zone. This amount of water is predicated on the assumption that the transition zone is oxidized (fO2–nickel–nickel oxide buffer) and, because their experimental setup imposed more reduced conditions (fO2 estimated to be close to the iron–wüstite buffer), they corrected their experimental data. Because several studies consider that the transition zone can be reduced and close to the IW buffer (McCammon 2005), Hirschmann (2006b) used Huang et al.'s data without the fO2 correction and
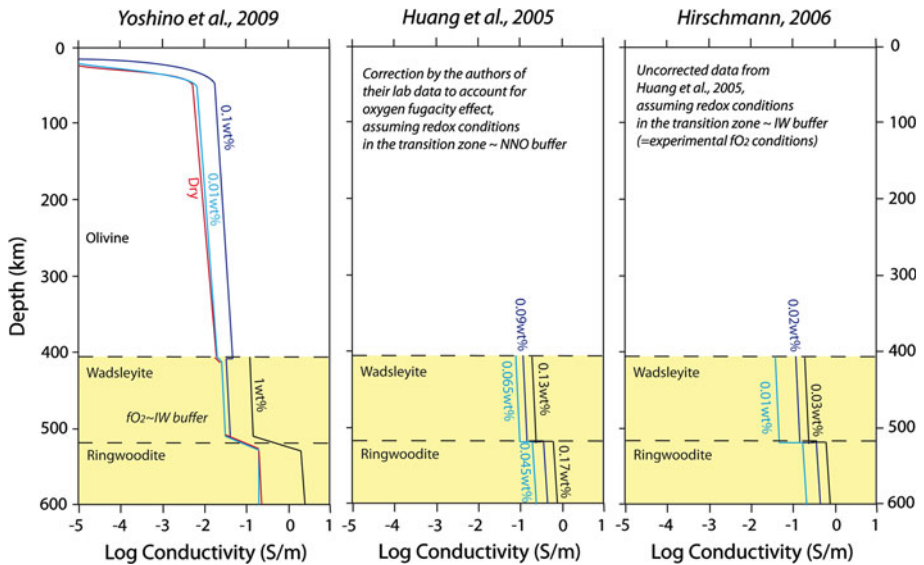
Fig. 8 Laboratory-based conductivity-depth profiles as a function of water contents (wt%). *Yellow* area corresponds to the transition zone. *Left* Yoshino et al. (2009), profile for the oceanic mantle geotherm. *Center* Huang et al. (2005), profiles corresponding to the best fits to field data in the transition zone below the Pacific Ocean. Calculations consider adiabatic temperatures (1,825–1,900 K in the transition zone). Laboratory data have been corrected by the authors [experimental fO$_2$–IW and the models are for fO$_2$–NNO (more oxidized mantle)]. *Right* Hirschmann (2006b), using equations from Huang et al. (2005) and the same adiabatic temperatures. Laboratory data have not been corrected (fO$_2$–IW buffer). As a result, a much lower water content is needed in the transition zone to obtain similar conductivities as Huang et al. (2005)

obtained, for similar *T* and *P* conditions, a best fit to MT soundings with only 0.01–0.03 wt% H$_2$O (Fig. 8).

3.1.2 Other Potentially Hydrous Minerals

Pyroxene and garnet are two other major phases in the Earth's mantle (Fig. 1) and may store significant amounts of water (e.g., Bell and Rossman 1992b; Mierdel et al. 2007; Katayama et al. 2003; Peslier 2010; Peslier et al. 2012), although recent laboratory experiments on olivine and pyroxene suggested that olivine is probably the main host of water at least in the deep upper mantle (Tenner et al. 2012). Quantifying the electrical response of pyroxene and garnet and the influence of water is needed to improve estimates of hydrogen that can be stored in a bulk mantle composition and place quantitative constraints on the conductivity profiles of the Earth's mantle. Only a few laboratory studies have been performed on hydrous pyroxenes: Dai and Karato (2009a) (0.0001 and 0.04 wt% H$_2$O at 8 GPa) and Zhang et al. (2012) (0.002–0.235 wt% H$_2$O at 3 GPa) for orthopyroxenes and Yang et al. (2011) and Yang and McCammon (2012) for clinopyroxenes (<0.0375 wt% H$_2$O, *P* range 0.6–1.2 GPa). The same comment can be made for hydrous garnet conductivity: Dai and Karato (2009b) (0.047, 0.016 and 0.0046 wt% H$_2$O, with pressure from 4 to 16 GPa) and Dai et al. (2012) (0.0465 wt% H$_2$O, with pressure from 1 to 4 GPa). Conduction models for hydrous pyroxene and garnet are shown in Table 3. No systematic study has yet investigated thoroughly the effect of composition on the conductivity of pyroxene or garnet. However, it seems that Fe-rich pyroxenes are more

Table 3 Conduction models for hydrous pyroxenes and garnets (C_w is the water content, T is the temperature (K), R is the universal gas constant (J mol^{-1} K^{-1}), A is the pre-exponential term, ΔH is the activation enthalpy, r is a constant, ΔV is the activation volume). See text for details

HYDROUS PYROXENE		
ORTHOPYROXENE *(Dai and Karato, 2009a):* $\sigma = A_H C_w^{\ r} exp\left(\frac{-\Delta H}{RT}\right)$		
A_H *(S/m)*	ΔH *(kJ/mol)*	r
$10^{2.6}$	82	0.62
ORTHOPYROXENE *(Yang et al., 2012):* $\sigma = A_H C_w^{\ r} exp\left(\frac{-\Delta H}{RT}\right)$		
A_H *(S/m)*	ΔH *(kJ/mol)*	r
$10^{3.83}$	81	0.90
ORTHOPYROXENE *(Zhang et al., 2012):* $\sigma = A_H C_w\ exp\left(\frac{-\left(\Delta H - \alpha C_w^{\frac{1}{3}}\right)}{RT}\right)$		
A_H *(S/m)*	ΔH *(kJ/mol)*	α
$10^{2.58}$	81	0.08
Fe-rich CLINOPYROXENE *(Yang et al., 2011):* $\sigma = A_H C_w^{\ r} exp\left(\frac{-\Delta H}{RT}\right)$		
A_H *(S/m)*	ΔH *(kJ/mol)*	r
$10^{3.56}$	71	1.13
Fe-rich CLINOPYROXENE *(Yang and McCammon, 2012):* $\sigma = A_H C_w^{\ r} exp\left(\frac{-\Delta H}{RT}\right)$		
A_H *(S/m)*	ΔH *(kJ/mol)*	r
$10^{3.67}$	73	0.94
HYDROUS GARNET		
PYROPE GARNET *(Dai and Karato, 2009b):* $\sigma = A_H C_w^{\ r} exp\left(\frac{-\Delta H}{RT}\right)$		
A_H *(S/m)*	ΔH *(kJ/mol)*	r
$10^{2.9}$	70	0.63
Py$_{73}$Alm$_{14}$Grs$_{13}$ GARNET with 465ppm water *(Dai et al., 2012):* $\sigma = A exp\left(-\frac{H + P\Delta V}{RT}\right)$		
A*(S/m))*	H *(kJ/mol)*	ΔV *(cc/mol)*
$10^{1.75}$	72.3	-1.4

conductive and present lower activation energy (Table 3). MT data interpretation involving a repartition of hydrogen between olivine, pyroxene and garnet (e.g., Jones et al. 2012) will probably be promoted in the near future and stimulate further laboratory investigations.

A process that probably contributes to enrich significantly the mantle with water is the subduction of the water-rich crust and lithospheric slab system (e.g., Ohtani et al. 2004). Slab assimilation and associated metamorphic processes lead to the formation of a suite of hydrous minerals in the upper mantle (>150–200 km) such as amphibole and phyllosilicates (talc, chlorite, antigorite) (Schmidt and Poli 1998; Fumagalli and Poli 2005; Grove et al. 2012). MT is a valuable tool to probe subduction zones (e.g., Evans et al. 2002; Brasse and Eydam 2008; Wannamaker et al. 2009; Worzewski et al. 2011), and constraining interpretations of conductive anomalies requires laboratory measurements on subduction-related materials. A few attempts have been made to investigate the electrical properties of subduction-related hydrous minerals (e.g., Tolland 1973; Shankland et al. 1997; Zhu et al. 2001; Guo et al. 2011; Reynard et al. 2011; Wang et al. 2012). As discussed by Reynard et al. 2011, several studies probably encountered issues (e.g., connected conductive metallic oxides in the antigorite sample in the study by Stesky and Brace 1973) related to the sample composition or potential analytical problems (Zhu et al. 2001) that may have altered the quality of the results. Further investigations with a characterization (SEM imaging) of the sample texture and the control of possible water loss from the sample during heating are therefore needed to strengthen the electrical database of hydrous minerals.

At higher pressure, dense hydrous magnesium silicates (DHMSs, including the so-called alphabet phases) have been suggested as a possible water reservoir in the Earth's mantle, with stabilities corresponding to depths >200 km (Williams and Hemley 2001 and references therein). For instance, phase equilibria of hydrous peridotite for conditions characteristic for subduction zones (e.g., Schmidt and Poli 1998) pointed out the presence of phase A, $Mg_7Si_2O_8(OH)_6$, which can store up to 11.8 wt% H_2O (e.g., Wunder 1998). Such phases, if present in significant amounts and assuming that their high water content provides them with a high conductivity, might explain some deep conductive anomalies in subduction zones. However, the conductivity of DHMS has not yet been documented. A major difficulty is synthesizing a quantity of these phases large enough to make a sample for conductivity measurements. If DHMSs are commonly observed in high-pressure runs, the lack of evidence of their presence at the surface of the Earth may cast doubt on their presence and abundance in the mantle.

3.1.3 Hydrous Silicate Melt

A wet mantle will initiate partial melting at lower temperatures than a dry mantle (Green 1973; Hirth and Kohlstedt 1996; Hirschmann 2006a), and several studies have investigated mineral/melt partition coefficients of hydrogen at relevant mantle conditions (e.g., Koga et al. 2003; Hauri et al. 2006; Aubaud et al. 2008; Tenner et al. 2009). These laboratory studies provide critical constraints on the water content and composition of melts that need to be considered as part of electrical studies in the laboratory.

Mid-ocean ridge basalt (MORB) source upper mantle, which is estimated to contain 50–250 wt ppm H_2O (e.g., Dixon et al. 1988; Danyushevsky et al. 2000; Saal et al. 2002), may not be wet enough to incite a global melt layer above the 410-km discontinuity (Tenner et al. 2012). However, at shallower depths, for example less than ∼150 km (<5 GPa), a possible interconnected melt (melt fraction of 0.1), and therefore geophysically detectable, may contain 3.2 wt% H_2O (Tenner et al. 2009). Ocean island basalt (OIB)

Fig. 9 Electrical conductivity of hydrous silicate melts and comparison with dry silicate melts (after Ni et al. 2011a). Data on basaltic melt are from Ni et al. (2011a), on phonolitic and phonotephritic melts from Pommier et al. (2008), on rhyolitic melt from Gaillard (2004) and on albitic melt from Ni et al. (2011b). *Numbers in brackets* are water contents in wt%
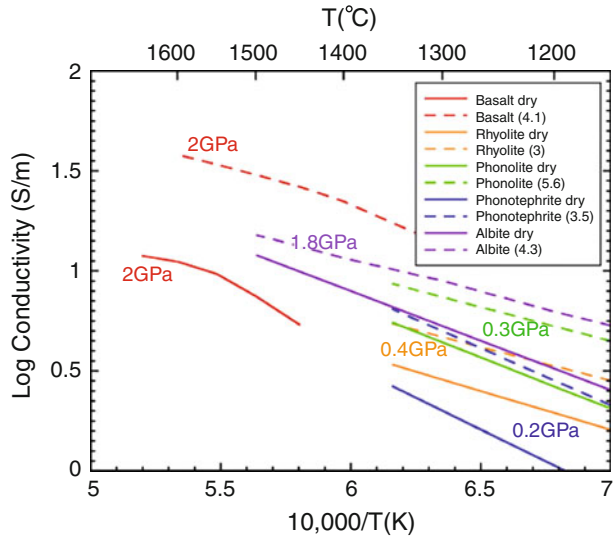
settings and residues of subducted slabs, which may contain 300–1,000 ppm bulk hydrogen (e.g., Dixon et al. 1997; Seaman et al. 2004), can exceed the peridotite H_2O storage capacity and incite localized hydrous partial melting (Tenner et al. 2012). These OIB source melts (3–20 wt% H_2O, Tenner et al. 2009) can be stable at great depth (higher than ~ 90 km, >3 GPa), and future electrical studies in the laboratory will probably aim to characterize their electrical response and compare it with MT surveys in these geographic areas. However, it is important to keep in mind that such hydrous melts will be clearly detected by MT surveys only if they are interconnected over a large scale (>hundreds of meters). Forward modeling of the response of electrical conductivity-depth profiles by Toffelmier and Tyburczy (2007) suggested that a hydrous melt layer at the top of the transition zone (410 km depth) occurs regionally in agreement with local seismic studies (e.g., Song et al. 2004), but is unlikely to be a global feature. Therefore, partially molten material in the upper mantle may be only intermittently detected using MT soundings.

Recent laboratory experiments have quantified the effect of water on silicate melt conductivity for a water content up to 6 wt% water and over the pressure range 0.3–2 GPa (Gaillard 2004; Pommier et al. 2008; Ni et al. 2011a) (Fig. 9). These data have been included as part of a general conductivity model of dry and hydrous silicate melts (available in the Web application SIGMELTS, Pommier and LeTrong 2011). Though limited, this electrical database of hydrous silicate melts allows the computation of their conductivity at crust and upper mantle conditions and its comparison with MT data acquired in contexts of high probability of hydrous melt, such as melting in subduction zones (Pommier and LeTrong 2011) (Fig. 10). Heating of solid mantle in the presence of H_2O-rich fluid released during slab dehydration at temperatures above the vapor-saturated solidus generates hydrous melt, whose water content can reach ~ 30 wt% (Hodges 1974; Mysen and Boettcher 1975). Its bulk conductivity, as imaged from MT profiles, contributes to place quantitative constraints on melt fraction and temperature for different scenarios (Fig. 10). For example, a melt with 30 wt% H_2O at 1,300 °C may have such a high conductivity that it would reproduce the field conductivity only with a melt proportion of 0.02 vol.%, which raises the question of its interconnectivity. At the same temperature, a melt fraction of 0.5 is necessary for the same basaltic melt containing 10 wt% H_2O.
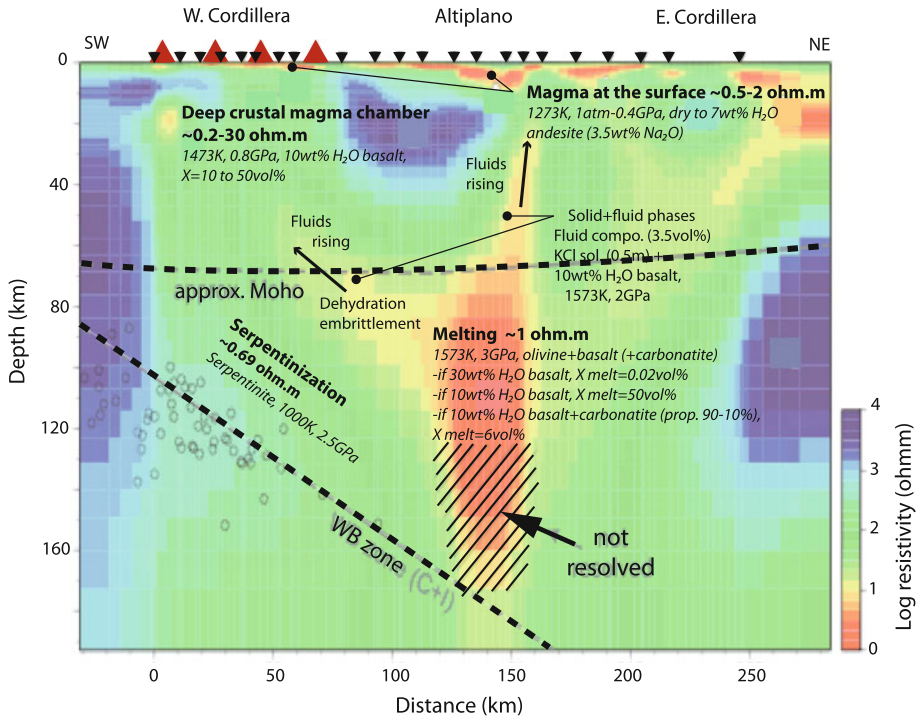
Fig. 10 Simple laboratory–field joint interpretation of the resistivity (=1/conductivity) of the Central Andes subduction zone (after Pommier and LeTrong 2011). MT profile is from Brasse and Eydam (2008), and laboratory-based constraints on resistivity values are from calculations using SIGMELTS. *WB* Wadati–Benioff zone, *circles* show the locations of earthquakes, locations. *Red* areas correspond to lower resistivities, that is, higher conductivities

However, at such a low degree of partial melting, melt composition may be richer in sodium (e.g., Hirschmann et al. 1999) and therefore more conductive than a basaltic melt. As illustrated in the MT image of Fig. 10, aqueous fluids and silicate melt being positively buoyant will then percolate upward by porous flow. Details about the role of water in subduction zones can be found in Grove et al. (2012) and references therein. Few quantitative electrical constraints can be placed on aqueous fluids because of a lack of laboratory measurements on free fluid phase under pressure and temperature. These experiments are very challenging (particularly regarding leaking issues of the conductivity cell), and only a few studies have been performed (e.g., Quist and Marshall 1968; Holzapfel 1969; Nesbitt 1993; Shimojuku et al. 2012). Recently, Reynard et al. 2011 proposed a conductivity model of saline fluid-rock mixtures that may stimulate experimental investigations.

Several MT studies have observed conductivity anomalies atop the transition zone (∼410 km depth) (e.g., Ichiki et al. 2001; Toffelmier and Tyburczy 2007), where the attenuation of seismic waves has been sometimes interpreted as the possible presence of partially molten mantle rocks (e.g., Hier-Majumder and Courtier 2011 and references therein). Beneath the French Alps and the North Pacific, conductivity is in the range 0.001–0.01 S/m (Utada et al. 2003; Tarits et al. 2004), whereas beneath North East China, and for another study in the North Pacific, it varies between 0.05 and 0.1 S/m (Lizarralde
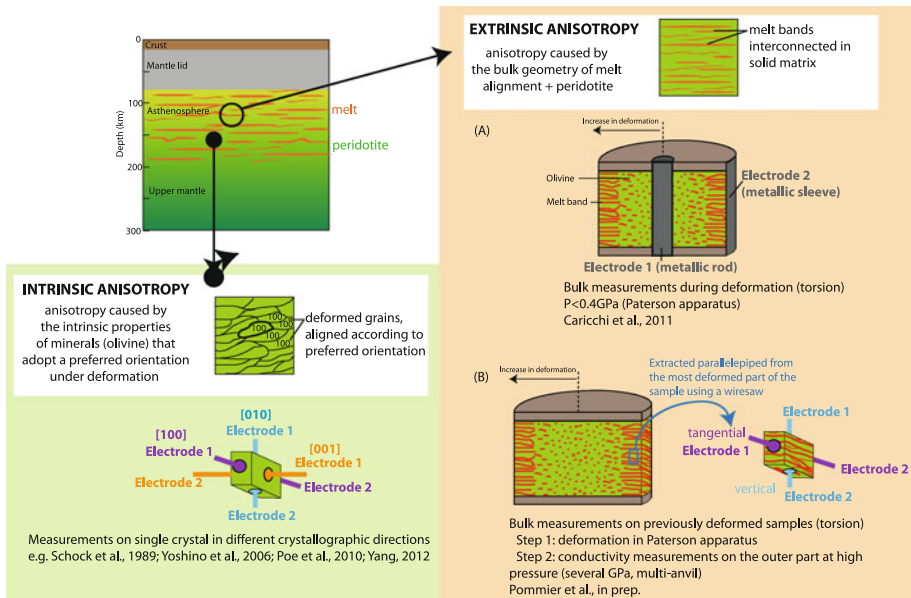
Fig. 11 Setups for laboratory investigation of electrical intrinsic and extrinsic anisotropies. Example of the asthenosphere (cross-section after Kawakatsu et al. 2009). Intrinsic anisotropy, caused by the preferred orientation of olivine grains, can be investigated at the scale of the laboratory by performing conductivity measurements on single crystals cut and oriented according to the main crystallographic directions (*left*). Extrinsic anisotropy, caused by the geometry of interconnected melt in a preferential direction, requires challenging laboratory setups that involve deformed partially molten materials (*right*)

et al. 1995; Ichiki et al. 2001). The lowest conductivity values (<0.01 S/m) can hardly be explained by the presence of hydrous melt since it would be more conductive. Tarits et al. (2004) explained their value of 0.01 S/m by the presence of water in olivine coming from slab dehydration. If there is melt, then it is present in a very small amount, in the form of isolated pockets that do not significantly influence the bulk conductivity. On the contrary, higher conductivities (>0.05 S/m) can be consistent with melt channels. For instance, laboratory measurements showed that a conductivity value of 0.1 S/m matches with the bulk conductivity of a basaltic melt (2 vol.%) at 1,300 °C interconnected with olivine (Caricchi et al. 2011).

3.2 Investigation of Electrical Anisotropy

As a second-order tensor, electrical conductivity can exhibit directionality at large and small scales. At large scales, electrical anisotropy can be caused by faults, dykes or highly deformed rocks. At a smaller scale, single crystals can present an intrinsic anisotropy (e.g., olivine). Field-scale anisotropy may be induced by variations in either mineralogy or crystallographic orientation, promoting multi-scale approaches. For instance, the anisotropy of a deformed rock (under shear) can be explained by the preferential orientation of its constituents [anisotropic grains resulting of a lattice-preferred orientation (LPO, a non-random orientation of the crystallographic axes of the constituent minerals) or a grain-shape-preferred orientation (SPO)], which in turn can be understood through laboratory investigations. A major current limit to cross-spatial-scale comparisons regarding electrical

anisotropy is that anisotropy is still not clearly resolved by electrical field measurements yet. In fact, how the trade-off is defined between anisotropy and heterogeneity in the inversion of MT data remains a challenge (Heinson and White 2005; Wannamaker 2005). It is also important to keep in mind that electrical anisotropy detected in MT does not necessarily imply an anisotropic fabric and that MT cannot easily make a distinction between fabric and structural anisotropies (Wannamaker 2005; Jones 2006; Evans 2012). An interpretation of MT data accounting for compositional and tectonic constraints is therefore necessary in order to pursue electrical anisotropy and its geological causes. As underlined by Eaton et al. (2004) and Jones (2006), seismic and MT measurements are both sensitive to crystallographic anisotropy, but both techniques may not probe the same anisotropic structures. Measured seismic anisotropy seems to be very sensitive to lattice-preferred orientation (LPO), while grain-shape-preferred orientation (SPO) may have a larger effect on electrical measurements (Ji et al. 1996). For a review of MT modeling of anisotropy, the reader is referred to Weidelt (1999), Pek and Santos (2002) and Martí, this volume.

This section focuses on how electrical anisotropy is investigated at the scale of the laboratory and what constraints it can place on field data for which electrical anisotropy has been established. Depending on whether anisotropy is intrinsic (crystallography) or extrinsic (e.g., caused by the bulk geometry of melt channels in peridotite), different setups have been proposed to measure in situ electrical anisotropy (Fig. 11). These experiments are challenging and point to several experimental issues, such as the precision in the orientation of the sample in comparison with the direction of the electrical current or the control of the texture especially when the sample is a partially molten material.

Laboratory studies of electrical anisotropy have focused primarily on olivine single crystals. These experiments are unquestionably critical to our understanding of electrical anisotropy in mantle minerals.[6] Measurements showed that electrical anisotropy on anhydrous olivine is weak and seems to be pressure and temperature dependent: At 1 bar, Schock et al. (1989) and Du Frane et al. (2005) obtained: $\sigma[010] <$ or $\sim \sigma[100] < \sigma[001]$ at $T > 1{,}200$ °C. Under pressure (<3 GPa), Yoshino et al. (2006) measured $\sigma[100] < \sigma[001] < \sigma[010]$ for $T > 800$ °C and $\sigma[010] < \sigma[001] < \sigma[100]$ for $T < 800$ °C. At 8 GPa, Poe et al. (2010) obtained $\sigma[010] < \sigma[001] \sim \sigma[100]$ for $T < 800$ °C (Fig. 12). Yoshino et al. (2006), Poe et al. (2010) and Yang (2012) conducted measurements on a hydrous olivine single crystals (Fig. 12). At 40 wt ppm, electrical anisotropy is not significant (Yang 2012). At 100 wt ppm H_2O, conduction along [100] is the highest and electrical anisotropy is greater at 1,000 wt ppm H_2O, with maximal conduction in the [010] direction (Poe et al. 2010). Measurements along the [100] axis are important to interpret field data in strain-induced deformation contexts since the resulting lattice-preferred orientation of dry olivine occurs in the [100] direction[7] (e.g., mantle rifting, Zhang and Karato 1995). In a context of wet olivine or in a melt-bearing system, the LPO will be different from that of dry olivine aggregates (Jung and Karato 2001; Holtzman et al. 2003). Anisotropy caused by olivine (dry or hydrous) has been suggested to explain field anomalies (e.g., Evans et al. 2005; Baba et al. 2006). Very conductive anomalies are yet a bit difficult to explain with this hypothesis. Existing laboratory results show that to account for the very conductive field

---

[6] Electrical and diffusion studies show that crystallographic defects are critical to create anisotropy. These defects can be point defects (e.g., vacancies), line defects (e.g., dislocations) and planar defects (e.g., stacking faults) (e.g., Skrotzy 1994; Dupas-Bruzek et al. 1998).

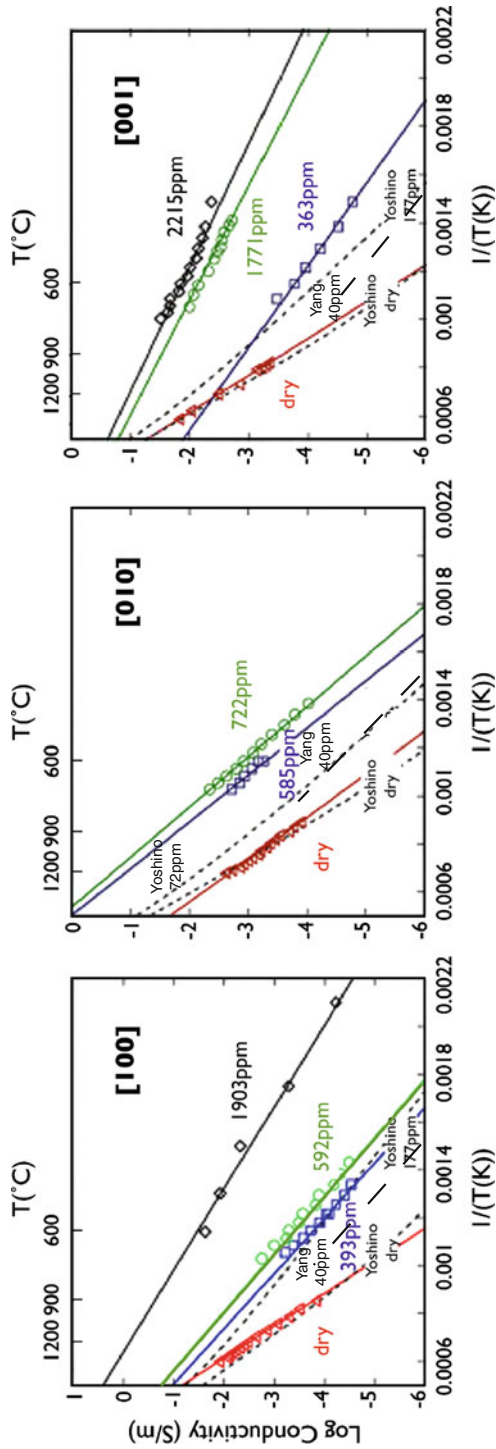[7] Dislocation creep is mainly due to the [100](010) slip system (Zhang and Karato 1995).

Fig. 12 Electrical anisotropy in olivine single crystal at various water contents (after Poe et al. 2010). Data from Poe et al. (2010) were collected at 8 GPa on San Carlos olivine crystals, data from Yoshino et al. (2006) (*dotted lines*) at 3 GPa on olivine crystals from China ($Mg_{0.92}Fe_{0.08}$)$2SiO_4$ and data from Yang (2012) at 1 GPa (*dashed lines*) on olivine crystals from Vietnam. *Solid lines* correspond to Arrhenian fits (dry) and derived Arrhenian fits (hydrous)
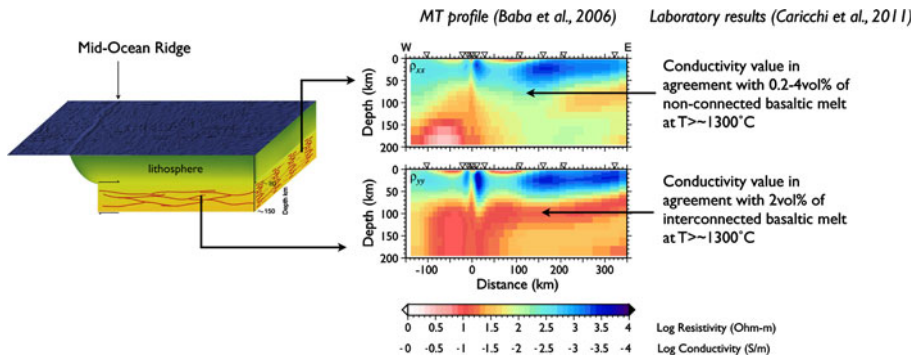
Fig. 13 Proposed interpretation of the electrical anisotropy below the East Pacific Rise based on laboratory experiments on deformed basalt + olivine samples by Caricchi et al. (2011). 3D drawing after Caricchi et al. (2011). MT profiles from Baba et al. (2006). *Upper* cross-section is ridge-parallel and *lower* cross-section is ridge-perpendicular

anomalies in the asthenosphere, anisotropy in hydrous olivine implies that olivine contains huge amounts of water ($\sim$ 1,000 wt ppm water at 8 GPa, see data by Poe et al. 2010), which are yet to be supported by data. Moreover, direct application of data of electrical anisotropy on single crystals to the field may be questionable. For instance, anisotropy in hydrous olivine strongly depends on shear-strain accumulation (Simpson and Tommassi 2005), and this is not taken into account as part of single-crystal studies. Another point concerns the effect of the presence of fluids that may possibly be present at the boundary between shear-deformed grains. How the presence of fluids would increase a bulk conductivity that is already enhanced by intrinsic anisotropy is poorly known.

The presence of anisotropic melt distribution has been suggested in mid-ocean ridge contexts (Daines and Kohlstedt 1997) as well as in some regions of the asthenosphere (Kawakatsu et al. 2009). These are contexts of high shear deformation, and the interconnectivity of melts under shear has been investigated at the scale of the laboratory (e.g., Zimmerman et al. 1999; Kohlstedt and Holtzman 2009). Based on laboratory electrical measurements on partially molten materials, Caricchi et al. (2011) suggested that the electrical anisotropy observed by Baba et al. 2006 below the East Pacific Rise may be explained by the presence of melt preferentially interconnected in the direction perpendicular to the ridge (Fig. 13). The anisotropy would be caused by the geometrical configuration of the rock rather than the intrinsic anisotropy of its constituents. Their experiments suggested that 2 vol.% of interconnected melt at 1,300 °C or higher T explains the MT data perpendicular to the ridge axis, whereas MT profiles parallel to the ridge are best explained by isolated melt pockets (0.2–4 vol.% of melt at $T >$ 1,300 °C). This interesting approach offered a new way to investigate extrinsic electrical anisotropy in the laboratory. Though improvements of the setup are possible and needed in order to work at higher pressure (>0.4 GPa), to monitor melt redistribution under static conditions and to measure the conductivity only on the most deformed part of the sample (Fig. 11), this study was the first to quantify the electrical anisotropy of a partially molten deformed material.

Note that the recent investigations of electrical intrinsic anisotropy of minerals other than olivine, for example orthopyroxene (Dai and Karato 2009a), quartz (Wang et al. 2010), clinopyroxene and plagioclase (Yang 2012), promise interesting future comparisons with olivine or melt to explain field anomalies.
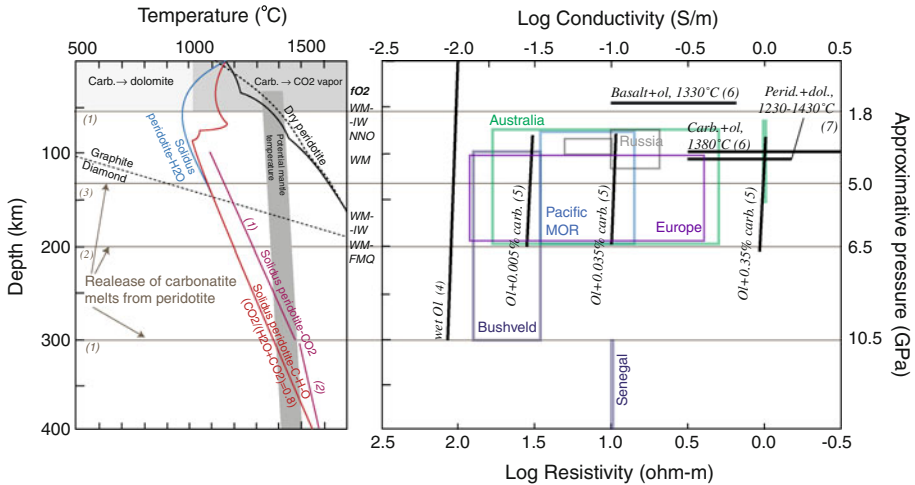
Fig. 14 Stability field (*left*) and electrical conductivity (*right*) of carbonated melts: comparison between laboratory and some field data in the asthenosphere. (*1*) Dasgupta and Hirschmann (2006); (*2*) Rohrbach and Schmidt (2011); (*3*) Frost and McCammon (2008); (*4*) Gaillard et al. (2008) using Yoshino et al. (2006); (*5*) Gaillard et al. (2008); (*6*) Yoshino et al. (2010); and (*7*) Yoshino et al. (2012). Phase-equilibria studies show that carbonatite melts are stable across most of the lithosphere, though the upper pressure limit of stability is still under debate, ranging between 300 and 130 km depth. Conductive asthenospheric regions are better explained by melts (silicate or carbonated) than by hydrous olivine (Ol) (150 wt ppm water). *Left* Dry peridotite solidus from Wyllie et al. (1990) (*full*) and Hirschmann (2010) (*dashed*); peridotite–H_2O and –CHO from Wyllie et al. (1990); peridotite–CO_2 solidus from (*1*) and (*2*); potential mantle temperature from (*2*). *Right* Field data are from Jones (1999) and references therein, Baba et al. (2006) and Evans et al. (2011)

3.3 Explaining Very High Conductive Anomalies in the Asthenosphere: The Carbonatite Hypothesis

Field conductivities of 0.1 S/m or higher are generally described as anomalously high (e.g., Shankland and Waff 1977). Depending on the considered datasets and temperature and redox conditions, hydrous olivine (containing several hundreds of wt ppm H_2O) may match with a value of 0.1 S/m, but it may also involve amounts of dissolved hydrogen that are well above the 50–250 wt ppm water estimated for the upper mantle (see Sect. 3.1.1). The high conductivity of silicate melt makes it a possible candidate if interconnected in the rock matrix, but its conductivity may imply huge melt fractions, particularly in the case of dry melt (>5 vol.%, Tyburczy and Waff 1983). Therefore, electrical investigations in the laboratory have focused on other potential candidates, especially carbonate materials.

Experiments on carbonatitic melts have been stimulated by several MT investigations that detected conductivities in the asthenosphere exceeding 0.1 S/m (e.g., Jegen and Edwards 1998; Evans et al. 2005, 2011; Baba et al. 2006). Experimental petrology studies (e.g., Wyllie et al. 1990; Dalton and Presnall 1998; Dasgupta and Hirschmann 2006; Dasgupta et al. 2007; Rohrbach and Schmidt 2011) have emphasized that carbonatitic melts are stable at the depths of these very conductive field anomalies (>2.5 GPa), therefore motivating the investigation of their electrical properties. The position of the solidus of carbonated peridotite below the mantle geotherm (Fig. 14) suggests a possible presence of melt up to ∼10 GPa, and experiments showed that 0.03–0.3 wt% carbonatite liquid can be produced below mid-ocean ridges up to 330 km depth (Dasgupta and

Hirschmann [2006]). In particular, thermodynamic modeling predicts that carbonatite melt can be stable at depths greater than 130–180 km assuming typical volatile contents (0.01 wt% water, 0.006 wt% CO_2) (Hirschmann [2010]). However, as pointed out by Hirschmann ([2010]), volatile-rich highly alkalic melt (H_2O, CO_2) is also stable at these depths and a small fraction of such a melt may also explain the high conductivity values in the upper mantle (low-velocity zone).

Only three studies performed electrical measurements on carbonatitic samples, and results are shown and compared to some field data in Fig. 14. Pioneering electrical measurements by Gaillard et al. ([2008]) showed that carbonatites are extremely conductive and suggested that only 0.1 vol.% of carbonate melt (compared to several vol.% of silicate melt) can match with the field conductivity in the asthenosphere. Yoshino et al. ([2010], [2012]) investigated the electrical conductivity of carbonatite melt-bearing peridotite up to 3 GPa and also measured very high conductivities attributed to a small amount of carbonatite melt, with an attempt to control melt distribution within the solid matrix. This amount is consistent with the fact that the dihedral angle of carbonatites is very low (28°, Hunter and McKenzie [1989]) and, as a result, the required melt fraction to have an interconnected melt is also very low. Also, carbonatite viscosity is lower than the viscosity of water (Dobson et al. [1996]) and Hammouda and Laporte [2000] demonstrated that its mobility into polycrystalline olivine is much higher than that of silicate melt. As illustrated in Fig. 14, conductivity results show that small amounts of carbonatite liquids (<0.3 wt%) can account for high conductivity anomalies in several regions in the upper mantle (130–330 km depth), in agreement with phase-equilibria constraints (e.g., Dasgupta and Hirschmann [2006]).

However, experiments on carbonatites are particularly challenging. First, there is a difficulty to maintain the sample from leaking out of the conductivity cell, due to its extremely low viscosity. Second, the experimental duration (a few tens of minutes) can dramatically affect measurements on melt–peridotite samples: It is actually very likely that, because of its high mobility, melt leaves the solid matrix and migrates toward the edge of the capsule before the sample reaches chemical equilibrium. This implies that bulk conductivity measurements are taken while both melt fraction and melt distribution evolve, increasing bulk inhomogeneity. Therefore, experimental strategy here requires one to make a choice between minimizing carbonatitic melt migration and reaching chemical equilibrium. It is likely that the recent investigations of the transition between carbonate and carbonated silicate melt (e.g., Dasgupta et al. [2007]) stimulate electrical measurements on silicate melts with CO_2 content as an experimental parameter. It can also be tempting to suggest the coexistence of silicate and carbonate melts to explain conductivity values that are higher than the conductivity of silicate melt alone. Actually, evidence for carbonate–silicate immiscibility has been observed in the field and experimentally in the laboratory (Lee and Wyllie [1997a], [b], [1998]). However, assumptions on geometry and connectivity of both phases, and thus on the choice of mixing law (i.e., of geometry) to compute the bulk conductivity of silicate and carbonate melts, require attention. Immiscibility experiments emphasized that silicate melt preferentially wets the solid matrix and, therefore, carbonate melt mobility is restricted, in contrast to expectations about its high mobility (Minarik [1998]). Such a result suggests that the addition of carbonate melt to silicate melt may not significantly increase the bulk conductivity.

It is interesting to note that, if carbonatitic melt is usually suggested to explain high conductive anomalies, it may also possibly account for lower conductivities depending on the geological context. For instance, Yoshino et al. ([2012]) suggested that the anomaly in the study by Baba et al. ([2010]) (constant value of ~0.03 S/m at depths >75 km) may correspond to 0.1 vol.% of carbonate melt and that the decrease in conductivity at

shallower depth could describe CO_2 release from the carbonate melt. As mentioned by Yoshino et al. (2012), future petrological studies of carbonate concentration in partially molten rocks in the upper mantle will help to place constraints on the melt fraction from MT profiles.

4 Current and Future Challenges to Improve the Quantitative Interpretation of MT Data

4.1 Caveats on How to Use Laboratory Data to Interpret MT Profiles

As suggested in the previous sections, electrical studies in the laboratory have produced a large dataset (though incomplete) of the conductivity data of Earth's materials as well as numerous conductivity models that do not always agree between each other. Moreover, and unfortunately, experimental details and subtleties related to experimental strategy that are mentioned in the literature (when available) are not always made accessible and well described to the reader. As a consequence, the integration of laboratory results into MT data interpretation can turn out to be difficult and somewhat challenging. Integrating laboratory-based models is, however, the only way to interpret thoroughly MT responses. Below is a non-exhaustive list of some important caveats that deserve being taken into account when laboratory data from the literature are used to interpret field results:

- Laboratory studies should provide information regarding the accuracy of the electrical measurements; in particular, the effect of noise on the electrical data (electrode effect, furnace effect) must be estimated (Pommier et al. 2010a). Regarding the technique itself, complex impedance spectroscopy is the most accurate technique currently available in the laboratory, allowing the discrimination of different conduction mechanisms.

- Laboratory studies should document the evolution of texture and composition of the sample before and after the experiments. This is particularly important for partially molten materials and for hydrous samples, since sample textural relaxation as well as dehydration will affect the bulk conductivity. Determination of water in minerals as accurate as possible is critical but current technique bias results in errors of up to 50 % in water content at times. The analysis of standards by different techniques (such as FTIR and SIMS) and laboratories is strongly advocated.

- Experimental conditions (temperature, pressure, composition, redox conditions, etc.) of selected laboratory studies should be relevant for the portion of the Earth's interior that has been probed using MT soundings and be consistent with petrological knowledge. For example, explaining conductive anomalies in the upper mantle by the presence of hydrous olivine requires considering water contents that are in agreement with estimates from petrology studies. A water content of 0.005–0.02 wt% has been estimated for the upper mantle, and higher water contents only concern the top of the transition zone (up to >0.4 wt%, Hirschmann et al. 2005). More generally, a robust interpretation of MT data cannot be achieved when using electrical laboratory data while neglecting petrological knowledge.

- Great caution must be exercised with the extrapolation of laboratory-based models to higher temperatures or pressures or water contents. For instance, when laboratory data are collected at low temperature on hydrous materials (in order to limit sample dehydration—see Fig. 7), an extrapolation of the results to the higher temperature

provided by the mantle geotherm can be a source of significant uncertainty. Extrapolation may be needed when the experimental dataset does not cover relevant conditions to the Earth's interior, but this must be clearly taken into account as part of data interpretation. Rounding experimental conductivity values as part of some conductivity modeling may dramatically increase error propagation in the computed data, too.

- It is important to keep in mind that conductivity equations proposed in laboratory studies are based on a set of experiments with specific experimental conditions (T, P, fO_2, duration, etc.). Some of these experimental conditions will not appear explicitly in the mathematical formulation of the equations, whereas they can become important parameters when applied to the field [see, for instance, the example of redox conditions on the conductivity model by Huang et al. (2005)] (Fig. 8). Therefore, using a laboratory-based conductivity model requires consideration of the experimental conditions at which data have been collected and making eventually a correction so conductivity data are relevant for the appropriate Earth's interior conditions.

4.2 Improvements of Laboratory and Field Techniques

In the laboratory, higher-quality electrical data will mostly depend on the careful chemical and physical characterization of the sample before and after each experiment, as well as the frequency range used for measurements, the cell design and the efficiency of the control of noise caused by electrodes and by the furnace. Details about the importance of the contribution of electrodes and its estimation (so that it can be deduced from the measured conductivity) can be found in Pommier et al. (2010a). Commonly used experimental strategy to minimize interference between the voltage applied to operate the furnace and the frequency signal to measure the sample's complex impedance is mentioned in Poe et al. (2010).

Obtaining conductivity data on fluids requires development of new conductivity setups that maintain the sample in the conductivity cell during measurements under pressure and temperature. Only a few attempts have been made and come principally from the material science community (e.g., Zimmerman et al. 1995, 2007), highlighting the need for furthered multi-disciplinary studies.

As emphasized in Sect. 2.1, new mixing solid–fluid models for representative geometries of the texture of materials in the Earth's mantle would greatly improve the integration of laboratory results as part of field data interpretation. Such models not only need electrical studies on multi-phase samples but would also benefit from laboratory investigations of sample deformation, permeability and porosity. Technical advances on the resolution of sample imaging (e.g., nano-tomography) will allow an extremely accurate characterization of the geometry of multi-phase materials that can greatly improve interconnectivity-dependent conductivity models.

Cross-spatial-scale comparisons can only be as good as constraints provided by both the laboratory and the field. Improvements in the MT technique will also contribute to further our understanding of the Earth's interior. High-quality data at very long periods are as challenging as a better treatment of data inversion or dimensionality (1D, 2D or 3D) as part of MT data analysis. Better estimates of the size and conductivity value of electrical field anomalies are requested to make the best use of laboratory data as part of MT profile interpretation. Among the points that directly influence the quality and relevance of cross-spatial-scale comparisons is the choice of the "best conductivity
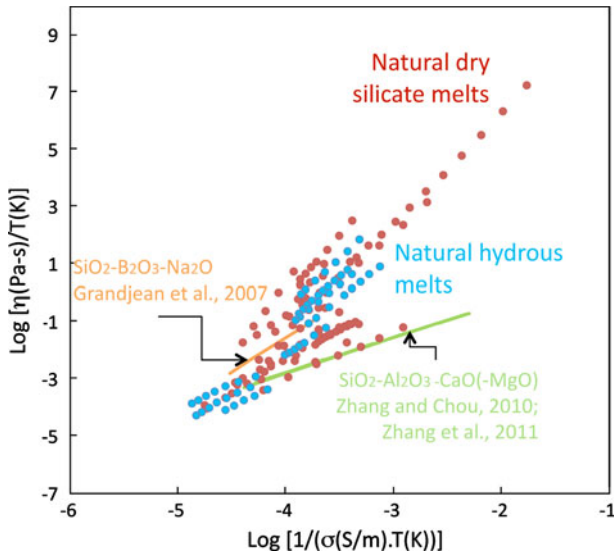
Fig. 15 Electrical conductivity (σ) versus viscosity (η) of complex (mostly natural) dry and hydrous silicate melts and comparison with synthetic compositions from Grandjean et al. (2007), Zhang and Chou (2010) (Pommier et al. 2013). Conductivities of natural melts are from experimental studies, and corresponding viscosities are calculated using the model of Giordano et al. (2008)

model" as part of MT data analysis (i.e., the final model that reproduces best the field data). In this preferred model, a conductivity value for an anomaly (such as melt) is arbitrarily chosen, independently from any consideration for laboratory results and petrological constraints on melt storage conditions and electrical response. The reader is referred to the books by Simpson and Bahr (2005) and by Chave and Jones (2012) for further details about issues that challenge the electromagnetic community.

4.3 Integration of Other Disciplines: Toward a Systematic Multi-disciplinary Approach

Cross-spatial-scale comparisons between MT profiles and conductivity studies in the laboratory greatly benefited from inputs from diffusion experiments, from deformation experiments, from seismic surveys and, more generally, from the knowledge of material science and geophysics. Each method being sensitive to specific parameters and probing different processes, a multi-disciplinary approach represents generally the opportunity to further the understanding of an Earth's interior probed by the conductivity tool only.

4.3.1 Including Rheology and Dynamics (Mixing and Convection) into MT Data Interpretation

A thorough interpretation of MT profiles should not only include laboratory results and petrological considerations, but—ideally—should also account for rheology and dynamics. For example, in a high melt-fraction magma reservoir, such characterization would allow determination of the timescale for buoyancy-driven motion and fractionation of crystals,
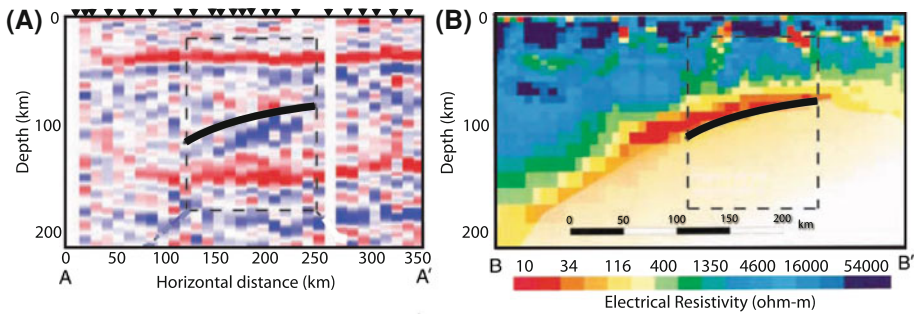
Fig. 16 Seismic (teleseismic receiver function) and MT profiles across the Slave craton, Canada (from Chen et al. 2009). In this Archean subduction zone, the main geophysical anomaly has been explained by the presence of graphite or phlogopite, related to metasomatic alteration. The *solid black line* underlines the base of the conductive anomaly. The seismic data (**a**) are particularly sensitive to the structure of the lithosphere, especially the position of the Moho (*top red* anomaly). MT data (**b**) seem to be more sensitive to products of alteration. Unfortunately, the lack of laboratory data on graphite and phlogopite prevents a more detailed interpretation of the conductive anomaly (in *red*)

melt segregation and magma mixing. Because viscosity governs any convective system, solid and/or fluid (Shaw 1965; Vetere et al. 2010; Karki and Stixrude 2010), relating melt electrical conductivity to melt viscosity represents an opportunity to improve the interpretation of electromagnetic field results.

In fact, the electrical conductivity and viscosity of silicate melts present an interesting correlation (Fig. 15), which has been previously investigated in simple systems by the material science community (e.g., Grandjean et al. 2007; Zhang and Chou 2010). Recently, a semiempirical model based on laboratory measurements of viscosity and conductivity has been developed for natural dry and hydrous silicate melts, with the aim of furthering geophysical data interpretation in contexts of high melt fraction (Pommier et al. 2013). Promisingly, this model can be used to convert melt conductivity into viscosity and vice versa for a defined melt composition and temperature, the values of the latter being constrained by petrological studies of the investigated region.

4.3.2 Integrating Seismic Profiles to Electrical Studies

Joint interpretation of models from seismic tomography and MT data was shown to be an efficient approach to determine lithologies in different contexts: subsurface (e.g., Bauer et al. 2012), crust (e.g., Hermance and Grillot 1970; Simpson and Warner 1998), active or ancient subduction systems (Chen et al. 2009; McGary et al. 2011), mid-ocean ridges (e.g., Key and Constable 2002), cratonic contexts (Jones et al. 2009) and transition zone (Utada et al. 2009). As suggested in the example presented Fig. 16, both techniques are not sensitive to the same parameters and therefore benefit from each other's information. Seismic wave velocities are very sensitive to composition change and therefore can constrain the crust–mantle boundary better than electromagnetics. It also seems that the seismic technique may help the detection of lattice-preferred orientation in deformed mantle materials, while MT soundings may be more sensitive to lineation and large-scale deformation patterns (Ji et al. 1996; Eaton et al. 2004) as well as conductive materials from alteration processes (e.g., graphite, phlogopite).

In a subduction context, slab serpentinization may be better detected on seismic profiles, while melting of the mantle wedge is clearly observed from MT results (Fig. 10, Brasse and Eydam 2008; McGary et al. 2011). Besides these differences, both techniques are affected by the presence of fluids, including melt, which can strengthen the identification of partially molten area on MT profiles that can consequently be interpreted in terms of composition, temperature and interconnectivity using laboratory measurements. The integration of seismic data to a field–laboratory electrical investigation provides a more robust interpretation than can be obtained using the conductivity tool only. A wider use of seismic profiles would considerably improve the interpretation of electrical data.

5 Concluding Remarks

Great progress has taken place in both field and laboratory studies of electrical properties of Earth materials. As part of future investigations, the opportunity is present for more directly bridging laboratory measurements to results from fundamentally different disciplines, such as petrology, geophysics and geodynamics.

Promoting the use of laboratory electrical data as part of a quantitative interpretation of MT results requires making laboratory measurements accessible to the geophysical community, through databases or laboratory-based modeling. But it also means that the limits and caveats of laboratory models should be acknowledged and made understandable, so that their use by the geophysical community can be made with more accuracy. Elaborated laboratory-based models combine experimental, thermodynamic and geophysical observations. However, as meaningful as they are to the geophysical community, these databases and models have to be coupled with petrological observations. Placing constraints on a field anomaly will only make sense if the conditions (pressure, temperature, composition, etc.) are relevant for the investigated area. For instance, the absolute value of olivine conductivity depends on the geological context, and history of the mineral and its electrical properties will not be exactly the same if it has an igneous or metamorphic origin (Duba and Constable 1993).

Compiling laboratory measurements also highlights what is lacking in the electrical database. Currently, conductivity data on fluids and hydrous minerals are particularly poorly constrained. This can be explained by the experimental difficulty to minimize the escape of fluids out of the conductivity cell during measurements, especially at high temperature and under pressure, highlighting the need for new conductivity setups and experimental strategies.

The missing link that exists between electromagnetic profiles and the understanding of the lithologies and processes that they probe is provided by laboratory experiments. This has been demonstrated for the Earth and could also be relevant for other planetary bodies, such as the Moon (Khan et al. 2006b; Khan et al. 2013).

References

Atekwana EA, Sauck WA, Werkema DD Jr (2000) Investigations of geoelectrical signatures at a hydro-carbon contaminated site. J Appl Geophys 44:167–180

Aubaud C, Hirschmann MM, Withers AC, Hervig RL (2008) Hydrogen partitioning between melt, clino-pyroxene, and garnet at 3 GPa in a hydrous MORB with 6 wt.% H_2O. Contrib Mineral Petrol 156:607–662

Baba K, Chave AD, Evans RL, Hirth G, Mackie RL (2006) Mantle dynamics beneath the East Pacific Rise at 17 degrees S: insights from the Mantle Electromagnetic and Tomography (MELT) experiment. J Geophys Res 111. doi:10.1029/2004jb003598

Baba K, Utada H, Gotob T-n, Kasayac T, Shimizua H, Tada N (2010) Electrical conductivity imaging of the Philippine Sea upper mantle using seafloor magnetotelluric data. Phys Earth Planet Int. doi:10.1016/j.pepi.2010.09.010

Bagdassarov N, Batalev V, Egorova V (2011) State of lithosphere beneath Tien Shan from petrology and electrical conductivity of xenoliths. J Geophys Res 116:B01202. doi:10.1029/2009JB007125

Bahr K (1997) Electrical anisotropy and conductivity distribution functions of fractal random networks and of the crust: the scale effect of connectivity. Geophys J Int 130:649–660

Bahr K, Olsen N, Shankland TJ (1993) On the combination of the magnetotelluric and the geomagnetic depth sounding method for resolving an electrical conductivity increase at 400 km depth. Geophys Res Lett 20:2937–2940

Baker DR, Freda C, Brooker RA, Scarlato P (2005) Volatile diffusion in silicate melts and its effects on melt inclusions. Ann Geophys 48(4–5):699–717

Banks RJ (1969) Geomagnetic variations and the electrical conductivity of the upper mantle. Geophys J R Astron Soc 17:457–487

Bauer K, Munoz G, Moeck I (2012) Pattern recognition and lithological interpretation of collocated seismic and magnetotelluric models using self-organizing maps. Geophys J Int 189:984–998

Bauerle JE (1969) Study of solid electrolyte polarization by a complex admittance method. J Phys Chem Solids 30:2657–2670

Bell DR, Rossman GR (1992a) Water in earth's mantle: the role of nominally anhydrous minerals. Science 255:1391–1397

Bell DR, Rossman GR (1992b) The distribution of hydroxyl in garnets from the subcontinental mantle in southern Africa. Contrib Mineral Petrol 111:161–178

Bell DR, Rossman GR, Maldener J, Endisch D, Rauch F (2003) Hydroxide in olivine: a quantitative determination of the absolute amount and calibration of the IR spectrum. J Geophys Res 108:B2105. doi:10.1029/2001JB000679

Berryman JG (1995) Mixture theories for rock properties. In: Ahrens TJ (ed) Handbook of physical constants. American Geophysical Union, New York

Bockris JOM, Kitchener JA, Ignatowicz S, Tomlinson JW (1952) Electric conductance in liquid silicates. Trans Faraday Soc 48:75–91

Bohlen SR, Boettcher AL (1982) The quartz-reversible-coesite transformation—a precise determination and the effects of other components. J Geophys Res 87(NB8):7073–7078

Brasse H, Eydam D (2008) Electrical conductivity beneath the Bolivian Orocline and its relation to sub-duction processes at the South American continental margin. J Geophys Res 113:B07109. doi:10.1029/2007JB005142

Caricchi L, Gaillard F, Mecklenburgh J, Le Trong E (2011) Experimental determination of electrical conductivity during deformation of melt-bearing olivine aggregates: implications for electrical anisotropy in the oceanic low velocity zone. Earth Planet Sci Lett. doi:10.1016/j.epsl.2010.11.041

Chave A, Jones AG (2012) The magnetotelluric method: theory and practice. Cambridge University Press, Cambridge

Chen C-W, Rondenay S, Evans RL, Snyder D (2009) Geophysical detection of relict metasomatism from an Archaean subduction zone. Science 326:1089–1091. doi:10.1126/science.1178477

Constable S (1993) Constraints on mantle electrical conductivity from field and laboratory measurements. J Geomagn Geoelectr 45:707–728

Constable S (2006) SEO3: a new model of olivine electrical conductivity. Geophys J Int 166:435–437

Constable S, Duba A (2002) Diffusion and mobility of electrically conducting defects in olivine. Phys Chem Miner 29:446–454

Constable S, Srnka LJ (2007) An introduction to marine controlled-source electromagnetic methods fro hydrocarbon exploration. Geophysics 72(2):WA3–WA12

Dai L, Karato S-I (2009a) Electrical conductivity of orthopyroxene: implications for the water content of the asthenosphere. Proc Jpn Acad Ser B 85:466–475

Dai L, Karato S-I (2009b) Electrical conductivity of pyrope-rich garnet at high temperature and high pressure. Phys Earth Planet Int 176:83–88

Dai L, Karato S-I (2009c) Electrical conductivity of wadsleyite under high pressures and temperatures. Earth Planet Sci Lett 287:277–283

Dai L, Li H, Hu H, Shan S (2008) Experimental study of grain boundary electrical conductivities of dry synthetic peridotite under high-temperature, high-pressure, and different oxygen fugacity conditions. J Geophys Res 113:B12211. doi:10.1029/2008JB005820

Dai L, Li H, Hu H, Shan S, Jiang J, Hui K (2012) The effect of chemical composition and oxygen fugacity on the electrical conductivity of dry and hydrous garnet at high temperatures and pressures. Contrib Mineral Petrol 163:689–700

Daines MJ, Kohlstedt DL (1997) Influence of deformation on melt topology in peridotites. J Geophys Res 102(B5):10257–10271

Dalton JA, Presnall DC (1998) Carbonatitic melts along the solidus of model lherzolite in the system CaO–MgO–Al$_2$O$_3$-SiO$_2$-CO$_2$ from 3 to 9 GPa. Contrib Mineral Petrol 131:123–135

Danyushevsky LV, Eggins SM, Falloon TJ, Christie DM (2000) H$_2$O abundance in depleted to moderately enriched mid-ocean ridge magmas; part I: incompatible behaviour, implications for mantle storage, and origin of regional variations. J Petrol 41:1329–1364

Dasgupta R, Hirschmann MM (2006) Melting in the earth's deep upper mantle caused by carbon dioxide. Nature 440:659–662

Dasgupta R, Hirschmann MM, Smith ND (2007) Partial melting experiments of peridotite + CO$_2$ at 3 GPa and genesis of alkalic ocean island basalts. J Petrol 48:2093–2124

De Bruin HJ, Franklin AD (1981) An impedance spectroscopy model for electron transfer reactions at an electrode/solid electrolyte interface. J Electroanal Chem 118:405–418

Demouchy S (2010a) Hydrogen diffusion in spinel grain boundaries and consequences for chemical homogenization in hydrous peridotite. Contrib Mineral Petrol. doi:10.1007/s00410-010-0512-4

Demouchy S (2010b) Diffusion of hydrogen in olivine grain boundaries and implications for the survival of water-rich zones in the Earth's mantle. Earth Planet Sci Lett 295:305–313

Demouchy S, Mackwell S (2003) Water diffusion in synthetic iron-free forsterite. Phys Chem Miner 30:486–494

Demouchy S, Mackwell S (2006) Mechanisms of hydrogen incorporation and diffusion in iron-bearing olivine. Phys Chem Miner 33:347–355

Dixon JE, Stolper E, Delaney JR (1988) Infrared spectroscopic measurements of CO$_2$ and H$_2$O in Juan de Fuca basaltic glasses. Earth Planet Sci Lett 90:87–104

Dixon JE, Clague DA, Wallace P, Poreda R (1997) Volatiles in alkalic basalts from the North Arch Volcanic Field, Hawaii: extensive degassing of deep submarine-erupted alkalic series lavas. J Petrol 38:911–939

Dobson DP, Brodholt JP (2000) The electrical conductivity and thermal profile of the earth's mid-mantle. Geophys Res Lett 27(15):2325–2328

Dobson DP, Jones AP, Rabe R, Sekine T, Kurita K, Taniguchi T, Kondo T, Kato T, Shimomura O, Urakawa S (1996) In situ measurement of viscosity and density of carbonate melts at high pressure. Earth Planet Sci Lett 143:207–215

Du Frane WL, Tyburczy JA (2012) Deuterium-hydrogen exchange in olivine: Implications for point defects and electrical conductivity. Geochem Geophys Geosyst 13(3):Q03004. doi:10.1029/2011GC003895

Du Frane WL, Roberts JJ, Toffelmier DA, Tyburczy JA (2005) Anisotropy of electrical conductivity in dry olivine. Geophys Res Lett 32:L24315. doi:10.1029/2005GL023879

Duba A (1976) Are laboratory electrical conductivity data relevant to the Earth? Acta Geodaet Geophys Montanist Acad Sci Hung 11(3–4):485–495

Duba A (1982) Limits to electrical measurements of silicates. In: Schreyer W (ed) High-pressure researches in geosciences. Schweizerbartische Verlagsbuchhandlung, Stuttgart, pp 375–381

Duba A, Constable S (1993) The electrical conductivity of lherzolite. J Geophys Res 98(B7):11885–11899

Duba A, Nicholls IA (1973) The influence of oxidation state on the electrical conductivity of olivine. Earth Planet Sci Lett 18:59–64

Duba A, Shankland TJ (1982) Free carbon and electrical conductivity in the earth's mantle. Geophys Res Lett 9(11):1271–1274

Duba A, Heard HC, Schock RN (1974) Electrical conductivity of olivine at high pressure and under controlled oxygen fugacity. J Geophys Res 79(11):1667–1673

Duba A, Piwinskii AJ, Heard HC, Schock RN (1976) The electrical conductivity of forsterite, enstatite and albite. In: Strens (ed) Physics and chemistry of minerals and rocks. Wiley-Interscience Publication. ISBN: 0471833681

Ducea MN, Park SK (2000) Enhanced conductivity from sulfide minerals, southern Sierra Nevada, California. Geophys Res Lett 27:2405–2408. doi:10.1029/2000GL011565

Dupas-Bruzek C, Sharp TG, Rubie DC, Durham WB (1998) Mechanisms of transformation and deformation in $Mg_{1.8}$ $Fe_{0.2}$ SiO_4 olivine and wadsleyite under non-hydrostatic stress. Phys Earth Planet Int 108:33–48

Eaton DW, Jones AG, Ferguson IJ (2004) Lithospheric anisotropy structure inferred from collocated teleseismic and magnetotelluric observations: Great Slave Lake shear zone, northern Canada. Geophys Res Lett 31. doi:10.1029/2004GL020939

Evans RL (2012) Conductivity of earth materials. In: Chave A, Jones AG (eds) The magnetotelluric method: theory and practice. Cambridge University Press, Cambridge, pp 50–95

Evans RL, Chave AD, Booker JR (2002) On the importance of offshore data for magnetotelluric studies of ocean-continent subduction systems. Geophys Res Lett 29(9). doi:10.1029/2001GL013960

Evans RL, Hirth G, Baba K, Forsyth D, Chave A, Mackie R (2005) Geophysical evidence from the MELT area for compositional controls on oceanic plates. Nature 437:249–252

Evans RL, Jones AG, Garcia X, Muller M, Hamilton M, Evans S, Fourie CJS, Spratt J, Webb S, Jelsma H, Hutchins D (2011) Electrical lithosphere beneath the Kaapvaal craton, southern Africa. J Geophys Res 116:B04105. doi:10.1029/2010JB007883

Faul UH, Toomey DR, Waff HS (1994) Intergranular basaltic melt is distributed in thin, elongated inclusions. Geophys Res Lett 21:29–32

Frost DJ, McCammon CA (2008) The redox state of earth's mantle. Annu Rev Earth Planet Sci 36:389–420

Frost BR, Fyfe WS, Tazaki K, Chan T (1989) Grain-boundary graphite in rocks and implications for high electrical conductivity in the lower crust. Nature 340:134

Fumagalli P, Poli S (2005) Experimentally determined phase relations in hydrous peridotites to 6.5 GPa and their consequences on the dynamics of subduction zones. J Petrol 46:555–578

Gaetani GA, Grove TL (2003) Experimental constraints on melt generation in the mantle wedge. In: Inside the subduction factory, Geophysical Monograph 138, pp 107–133

Gaillard F (2004) Laboratory measurements of electrical conductivity of hydrous and dry silicic melts under pressure. Earth Planet Sci Lett 218(1–2):215–228. doi:10.1016/S0012-821X(03)00639-3

Gaillard F, Iacono Marziano G (2005) Electrical conductivity of magma in the course of crystallization controlled by their residual liquid composition. J Geophys Res 110:B06204. doi:10.1029/2004JB003282

Gaillard F, Marki M, Iacono-Marziano G, Pichavant M, Scaillet B (2008) Carbonatite melts and electrical conductivity in the asthenosphere. Science 32:1363–1365

Giordano D, Russell JK, Dingwell DB (2008) Viscosity of magmatic liquids: a model. Earth Planet Sci Lett 271:123–134

Glover PWJ, Pous J, Queralt P, Munoz JA, Liesa M, Hole MJ (2000) Integrated two-dimensional lithospheric conductivity modelling in the pyrenees using field-scale and laboratory measurements. Earth Planet Sci Lett 178:59–72

Grandjean A, Malki M, Simonnet C, Manara D, Penelon B (2007) Correlation between electrical conductivity, viscosity, and structure in borosilicate glass-forming melts. Phys Rev B 75:054112. doi:10.1103/PhysRevB.75.054112

Grant FS, West GF (1965) Introduction to the electrical methods. In: Shrock RR (ed) Interpretation theory in applied geophysics. McGraw-Hill, New York, pp 385–401

Green DH (1973) Experimental melting studies on a model upper mantle composition at high-pressure under water-saturated and water-undersaturated conditions. Earth Planet Sci Lett 19:37–53

Grove TL, Till CB, Krawczynski MJ (2012) The role of H_2O in subduction zone magmatism. Annu Rev Earth Planet Sci 40:413–439

Guéguen Y, Palciauskas V (1994) Introduction to the physics of rocks. Princeton University Press, Princeton

Guéguen Y, Chelidze T, Le Ravalec M (1997) Microstructures, percolation thresholds, and rock physical properties. Tectonophysics 279:23–35

Guo X, Yoshino T, Katayama I (2011) Electrical conductivity anisotropy of deformed talc rocks and serpentinites at 3 GPa. Phys Earth Planet Int 188:69–81

Hammouda T, Laporte D (2000) Ultrafast mantle impregnation by carbonatite melt. Geology 28:283–285

Hashin Z, Shtrikmann S (1962) A variational approach to the theory of the effective magnetic permeability of multiphase materials. J Appl Phys 33:3125–3131

Hauri EH, Gaetani GA, Green TH (2006) Partitioning of water during melting of the earth's upper mantle at H_2O-undersaturated conditions. Earth Planet Sci Lett 248:715–734

Heinson G, White A (2005) Electrical resistivity of the Northern Australian lithosphere: crustal anisotropy or mantle heterogeneity? Earth Planet Sci Lett 232:157–170

Hermance JF, Grillot LR (1970) Correlation of magnetotelluric, seismic, and temperature data from Southwest Iceland. J Geophys Res 75(32):6582–6591

Hernlund J, Leinenwewber K, Locke D, Tyburczy JA (2006) A numerical model for steady-state temperature distributions in solid-medium high-pressure cell assemblies. Am Mineral 91:295–305

Hier-Majumder S, Courtier A (2011) Seismic signature of small melt fraction atop the transition zone. Earth Planet Sci Lett. doi:10.1016/j.epsl.2011.05.055

Hirschmann MM (2006a) Water, melting, and the deep earth H_2O cycle. Annu Rev Earth Planet Sci 34:629–653

Hirschmann MM (2006b) A wet mantle conductor? Arising from: X. Huang, Y. Xu & S. Karato Nature 434, 746–749 (2005). Nature. doi:10.1038/nature04528

Hirschmann MM (2010) Partial melt in the oceanic low velocity zone. Phys Earth Planet Int 179:60–71

Hirschmann MM, Ghiorso MS, Stolper EM (1999) Calculation of peridotite partial melting from thermodynamic models of minerals and melts. II. Isobaric variations in melts near the solidus and owing to variable source composition. J Petrol 40(2):297–313

Hirschmann MM, Aubaud C, Withers AC (2005) Storage capacity of H_2O in nominally anhydrous minerals in the upper mantle. Earth Planet Sci Lett 236:167–181

Hirth G, Kohlstedt DL (1996) Water in the oceanic upper mantle: implications for rheology, melt extraction and the evolution of the lithosphere. Earth Planet Sci Lett 144:93–108

Hirth G, Evans RL, Chave AD (2000) Comparison of continental and oceanic mantle electrical conductivity: is the Archean lithosphere dry? Geochim Geophys Geosyst 1. doi:10.1029/2000GC000048

Hodges FN (1974) The solubility of H_2O in silicate melts. Year b Carnegie Instn Wash 73:251–255

Holloway JR, Pan V, Gudmundsson G (1992) High-pressure fluid-absent melting experiments in the presence of graphite: oxygen fugacity, ferric/ferrous ratio and dissolved CO_2. Eur J Mineral 4:105–114

Holtzman BK, Kohlstedt DL, Zimmerman ME, Heidelbach F, Hiraga T, Hustoft J (2003) Melt segregation and strain partitioning: implications for seismic anisotropy and mantle flow. Science 301:1227–1230

Holzapfel WB (1969) Effect of pressure and temperature on the conductivity and ionic dissociation of water up to 10 kbar and 1000°C. J Chem Phys 50:4424–4428

Huang XG, Xu YS, Karato SI (2005) Water content in the transition zone from electrical conductivity of wadsleyite and ringwoodite. Nature 434:746–749

Huebner JS, Dillenburg RG (1995) Impedance spectra of hot, dry silicate minerals and rock: qualitative interpretation of spectra. Am Mineral 80:46–64

Hunter RH, McKenzie D (1989) The equilibrium geometry of carbonate melts in rocks of mantle composition. Earth Planet Sci Lett 92:347–356

Ichiki M, Uyeshima M, Utada H, Zhao G, Tang J, Ma M (2001) Upper mantle conductivity structure of the back-arc region beneath northeastern China. Geophys Res Lett 28:3773–3776

Inoue T, Weidner DJ, Northrup PA, Parise JB (1998) Elastic properties of hydrous ringwoodite (γ-phase) on Mg_2SiO_4. Earth Planet Sci Lett 160:107–113

Inoue T, Wada T, Sasaki R, Yurimoto H (2010) Water partitioning in the earth's mantle. Phys Earth Planet Int 183:245–251

Jacobsen SD, Smyth JR, Spetzler H, Holl CM, Frost DJ (2004) Sound velocities and elastic constants of iron-bearing hydrous ringwoodite. Phys Earth Planet Int 143–144:47–56

Jambon A (1994) Earth degassing and large-scale geochemical cycling of volatile elements. In: Volatiles in magmas. Rev Mineral 30:479–517

Jegen M, Edwards RN (1998) Electrical properties of a 2D conductive zone under the Juan de Fuca ridge. Geophys Res Lett 25:3647–3650

Ji S, Rondenay S, Mareschal L, Senechal G (1996) Obliquity between seismic and electrical anisotropies as a potential indicator of movement sense for ductile shear zones in the upper mantle. Geology 24:1033–1036

Jones AG (1999) Imaging the continental upper mantle using electromagnetic methods. Lithos 48:57–80

Jones AG (2006) Electromagnetic interrogation of the anisotropic earth: looking into the earth with polarized spectacles. Phys Earth Planet Int 158:281–291

Jones AG, Dumas I (1993) Electromagnetic images of a volcanic zone. Phys Earth Planet Sci 81:289–314

Jones AG, Gough DI (1995) Electromagnetic images of crustal structures in southern and central Canadian Cordillera. Can J Earth Sci 32(10):1541–1563

Jones AG, Evans RL, Muller MR, Hamilton MP, Miensopust MP, Garcia X, Cole P, Ngwisanyi T, Hutchins D, Fourie CJS, Jelsma H, Evans S, Aravanis T, Pettit W, Webb S, Wasborg J, The SAMTEX Team (2009) Area selection for diamonds using magnetotellurics: examples from southern Africa. Lithos 112S:83–92

Jones AG, Fullea J, Evans RL, Muller MR (2012) Water in cratonic lithosphere: calibrating laboratory-determined models of electrical conductivity of mantle minerals using geophysical and petrological observations. Geochem Geophys Geosyst V13(1):Q06010. doi:10.1029/2012GC004055

Jung H, Karato S (2001) Water-induced fabric transitions in olivine. Science 293:1460–1463

Karato S (1990) The role of hydrogen in the electrical conductivity of the upper mantle. Nature 347:272–273. doi:10.1038/347272a0

Karato S (2006) Remote sensing of hydrogen in earth's mantle. In: Keppler H, Smyth J (eds) Water in nominally anhydrous minerals. Mineralogical Society of America, Washington, DC, pp 343–375

Kariya KA, Shankland TJ (1983) Electrical conductivity of dry lower crustal rocks. Geophysics 48:52–61

Karki BB, Stixrude L (2010) Viscosity of MgSiO₃ liquid at earth's mantle conditions: implications for an early magma ocean. Science 328:740–742

Katayama I, Hirose K, Yurimoto H, Nakashima S (2003) Water solubility in majoritic garnet in subducting oceanic crust. Geophys Res Lett 30:2155. doi:10.1029/2003GL018127

Kawakatsu H, Kumar P, Takei Y, Shinohara M, Kanazawa T, Araki E, Suyehiro K (2009) Seismic evidence for sharp lithosphere–asthenosphere boundaries of oceanic plates. Science 324:499–502

Kelbert A, Schultz A, Egbert G (2009) Global electromagnetic induction constraints on transition-zone water content variations. Nature 460. doi:10.1038/nature08257

Key K, Constable S (2002) Broadband marine MT exploration of the East Pacific Rise at 9°50′N. Geophys Res Lett 29. doi:10.1029/2002GL016035

Khan A, Shankland TJ (2012) A geophysical perspective on mantle water content and melting: inverting electromagnetic sounding data using laboratory-based electrical conductivity profiles. Earth Planet Sci Lett 317–318:27–43

Khan A, Connolly JAD, Olsen N (2006a) Constraining the composition and thermal state of the mantle beneath Europe from inversion of long-period electromagnetic sounding data. J Geophys Res 111:B10102. doi:10.1029/2006JB004270

Khan A, Connolly JAD, Olsen N, Mosegaard K (2006b) Constraining the composition and thermal state of the moon from an inversion of electromagnetic lunar day-side transfer functions. Earth Planet Sci Lett 248:579–598

Khan A, Kuvshinov, Semenov A (2011) On the heterogeneous electrical conductivity structure of the Earth's mantle with implications for transition zone water content, J Geophys Res 116:B01103.doi:10.1029/2010JB007458

Khan A, Pommier A, Connolly JAD (2013) On the presence of a titanium-rich melt-layer in the deep lunar interior lunar and planetary science conference XLIV, abstract 1272. Lunar and Planetary Institute, Houston

Khitarov N, Slutskii B (1965) The effect of pressure on the melting temperatures of albite and basalt (based on electroconductivity measurements). Geochem Int 2:1034–1041

Koga K, Hauri E, Hirschmann M, Bell D (2003) Hydrogen concentration analyses using SIMS and FTIR: comparison and calibration for nominally anhydrous minerals. Geochem Geophys Geosyst. doi:10.1029/2002GC000378

Kohlstedt DL, Holtzman BK (2009) Shearing melt out of the earth: an experimentalist's perspective on the influence of deformation on melt extraction. Annu Rev Earth Planet Sci 37:561–593

Kohlstedt DL, Mackwell SJ (1998) Diffusion of hydrogen and intrinsic point defects in olivine. Z Phys Chem 207:147–162

Kohlstedt DL, Mackwell SJ (1999) Solubility and diffusion of "water" in silicate minerals. In: Wright Kate, Catlow Richard (eds) Microscopic properties and processes in minerals. Kluwer, Dordrecht, pp 539–559

Kohlstedt DL, Mackwell SJ (2010) Strength and deformation of planetary lithospheres. In: Watters TR, Schultz RA (eds) Planetary tectonics. Cambridge University, Cambridge, pp 397–456

Kohlstedt DL, Keppler H, Rubie DC (1996) Solubility of water in the α, β and γ phases of (Mg,Fe)₂SiO₄. Contrib Mineral Petrol 123:345–357. doi:10.1007/s004100050161

Kurtz RD, Craven JA, Niblett ER, Stevens RA (1993) The conductivity of the crust and upper mantle beneath Kapuskasing uplift: electrical anisotropy in the upper mantle. Geophys J Int 113:483–498

Le Pape F, Jones AG, Vozar J, Wenbo W (2012) Penetration of crustal melt beyond the Kunlun Fault into northern Tibet. Nat Geosci. doi:10.1038/NGEO1449

Lebedev EB, Khitarov NI (1964) Dependence of the beginning of melting of granite and the electrical conductivity of its melt on high water vapor pressure. Geochem Int 1:193–197

Lee W-J, Wyllie PJ (1997a) Liquid immiscibility between nephelinite and carbonatite from 2.5 to 1.0 GPa compared with mantle melt compositions. Contrib Mineral Petrol 127:1–12

Lee W-J, Wyllie PJ (1997b) Liquid immiscibility in the join NaAlSiO₄–NaAlSi₃O₈–CaCO₃ at 1.0 GPa: implications for crustal carbonatites. J Petrol 38:1113–1135

Lee W-J, Wyllie PJ (1998) Processes of crustal carbonatite formation by liquid immiscibility and differentiation, elucidated by model systems. J Petrol 39(11–12):2005–2013

Leinenweber KD, Tyburczy JA, Sharp TG, Soignard E, Diedrich T, Petuskey WB, Wang Y, Mosenfelder JL (2012) Cell assemblies for reproducible multi-anvil experiments (the COMPRES assemblies). Am Mineral 97:353–368

Lindsley DH, Dixon SA (1976) Diopside–enstatite equilibria at 850 to 1400°C, 5 to 35 kb. Am J Sci 276(10):1285–1301

Lizarralde D, Chave A, Hirth G, Schultz A (1995) Northeastern Pacific mantle conductivity profile from long-period magnetotelluric sounding using Hawaii-to-California submarine cable data. J Geophys Res 100(B9):17837–17854

Mackwell SJ, Kohlstedt DL (1990) Diffusion of hydrogen in olivine: implications for water in the mantle. J Geophys Res 95:5079–5088

Mackwell SJ, Kohlstedt DL, Paterson MS (1985) The role of water in the deformation of olivine single crystals. J Geophys Res 90:11319–11333

Manthilake MAGM, Matsuzaki T, Yoshino T, Yamashita S, Ito E, Katsura T (2009) Electrical conductivity of wadsleyite as a function of temperature and water content. Phys Earth Planet Int 174:10–18

Manzella A, Volpi G, Zaja A, Meju M (2004) Combined TEM-MT investigation of shallow-depth resistivity structure of Mt. Somma-Vesuvius. J Volcanol Geotherm Res 131(1–2):19–32. doi:10.1016/S0377-0273(03)00313-5

Martí A (this volume) The role of electrical anisotropy in magnetotelluric responses: From modelling and dimensionality analysis to inversion and interpretation

McCammon C (2005) The paradox of mantle redox. Science 308:807–808

McGary RS, Rondenay S, Evans RL, Abers GA, Wannamaker PE (2011) A joint geophysical investigation of the Cascadia subduction system in central Washington using dense arrays of passive seismic and magnetotelluric station data. Abstract V54B-03, AGU Fall Meeting, CA

Meju MA (2002) Geoelectromagnetic exploration for natural resources: models, case studies and challenges. Surv Geophys 23(203):133–205

Michael PJ (1995) Regionally distinctive sources of depleted MORB: evidence from trace elements and H_2O. Earth Planet Sci Lett 131:301–320

Mierdel K, Keppler H, Smyth JR, Langenhorst F (2007) Water solubility in aluminous orthopyroxene and the origin of earth's asthenosphere. Science 315:364–368

Minarik WG (1998) Complications to carbonate melt mobility due to the presence of an immiscible silicate melt. J Petrol 39(11–12):1965–1973

Moynihan CT (1998) Description and analysis of electrical relaxation data for ionically conducting glasses and melts. Solid State Ionics 105:175–183

Mysen BO, Boettcher AL (1975) Melting of a hydrous mantle: I. Phase relations of natural peridotite at high pressures and temperatures with controlled activities of water, carbon dioxide, and hydrogen. J Petrol 16:520–548

Nabighian MN, Asten MW (2002) Metalliferous mining geophysics—state of the art in the last decade of the 20th century and the beginning of the new millennium. Geophysics 67(3):964–978

Nesbitt BE (1993) Electrical resistivities of crustal fluids. J Geophys Res 98:4301–4310

Ni H, Keppler H, Behrens H (2011a) Electrical conductivity of hydrous basaltic melts: implications for partial melting in the upper mantle. Contrib Mineral Petrol 162:637–650

Ni H, Keppler H, Manthilake MAGM, Katsura T (2011b) Electrical conductivity of dry and hydrous Na-$AlSi_3O_8$ glasses and liquids at high pressures. Contrib Mineral Petrol. doi:10.1007/s00410-011-0608-5

Nover G (2005) Electrical properties of crustal and mantle rocks—a review of laboratory measurements and their explanation. Surv Geophys 26:593–651. doi:10.1007/s10712-005-1759-6

Ogawa Y, Mishina M, Goto T, Satoh H, Oshiman N, Kasaya T, Takahashi Y, Nishitani T, Sakanaka S, Uyeshima M, Takahashi Y, Honkura Y, Matsushima M (2001) Magnetotelluric imaging of fluids in intraplate earthquake zones, NE Japan back arc. Geophys Res Lett 28(19):3741–3744

Ohta, K Onoda, S Hirose, K, Sinmyo R, Shimizu K, Sata N, Ohishi Y, Yasuhara A (2008) The electrical conductivity of post-perovskite in Earth's D" layer. Science 320:89–91

Ohtani E, Litasov K, Hosoya T, Kubo T, Kondo T (2004) Water transport into the deep mantle and formation of a hydrous transition zone. Phys Earth Planet Int 143–144:255–269

Olhoeft GR (1981) Electrical properties of granite with implications for the lower crust. J Geophys Res 86(B2):931–936

Parman SW, Dann JC, Grove TL, de Wit MJ (1997) Emplacement conditions of komatiite magmas from the 3.49 Ga Komati Formation, Barberton Greenstone Belt, South Africa. Earth Planet Sci Lett 150:303–323

Parsons RA, Nimmo F, Hustoft JW, Holtzman BK, Kohlstedt DL (2008) An experimental and numerical study of surface tension-driven melt flow. Earth Planet Sci Lett 267:548–557

Pek J, Santos FAM (2002) Magnetotelluric impedances and parametric sensitivities for 1-D anisotropic layered media. Comput Geosci 28:939–950

Peslier AH (2010) A review of water contents of nominally anhydrous natural minerals in the mantles of Earth, Mars and the Moon. J Volcanol Geotherm Res 197:239–258

Peslier AH, Luhr JF (2006) Hydrogen loss from olivines in mantle xenoliths from Simcoe (USA) and Mexico: mafic alkalic magma ascent rates and water budget of the sub-continental lithosphere. Earth Planet Sci Lett 242:302–319

Peslier AH, Woodland AB, Wolff JA (2008) Fast kimberlite ascent rates estimated from hydrogen diffusion profiles in xenolithic olivines from Southern Africa. Geochim Cosmochim Acta 72:2711–2722

Peslier AH, Woodland AB, Bell DR, Lazarov M, Lapen TJ (2012) Metasomatic control of water contents in the Kaapvaal cratonic mantle. Geochim Cosmochim Acta 97:213–246

Piwinskii AJ, Duba A (1974) High temperature electrical conductivity of albite. Geophys Res Lett 1:209–211

Poe BT, Romano C, Nestola F, Smyth JR (2010) Electrical conductivity anisotropy of dry and hydrous olivine at 8 GPa. Phys Earth Planet Int 181:103–111

Pommier A, LeTrong E (2011) ''SIGMELTS'': a web portal for electrical conductivity calculations in geosciences. Comput Geosci. doi:10.1016/j.cageo.2011.01.002

Pommier A, Gaillard F, Pichavant M, Scaillet B (2008) Laboratory measurements of electrical conductivities of hydrous and dry Mount Vesuvius melts under pressure. J Geophys Res 113:B05205. doi:10.1029/2007JB005269

Pommier A, Gaillard F, Malki M, Pichavant M (2010a) Methodological re-evaluation of the electrical conductivity of silicate melts. Am Mineral 95:284–291

Pommier A, Gaillard F, Pichavant M (2010b) Time-dependent changes of the electrical conductivity of basaltic melts with redox state. Geochim Cosmochim Acta 74:1653–1671

Pommier A, Tarits P, Hautot S, Pichavant M, Scaillet B, Gaillard F (2010c) A new petrological and geophysical investigation of the present-day plumbing system of Mount Vesuvius. Geochem Geophys Geosyst 11:Q07013. doi:10.1029/2010GC003059

Pommier A, Evans RL, Key K (2011) Joint-modeling of the viscosity and the electrical conductivity of silicate and carbonatitic melts and implications for geophysical data interpretation. Abstract V22D-08, AGU Fall Meeting, CA

Pommier A, Evans RL, Key K, Tyburczy J, Mackwell S, Elsenbeck J (2013) Prediction of silicate melt viscosity from electrical conductivity: a model and its geophysical implications. G-Cubed 14. doi:10.1002/2012GC004467

Quist AS, Marshall WL (1968) Electrical conductances of aqueous sodium chloride solutions from 0 to 800 degrees and at pressures to 4000 bars. J Phys Chem 72:684–703

Rauen A, Lastovickova M (1995) Investigation of electrical anisotropy in the deep borehole KTB. Surv Geophys 16:37–46

Reynard B, Mibe K, Van de Moortèle B (2011) Electrical conductivity of the serpentinised mantle and fluid flow in subduction zones. Earth Planet Sci Lett 307:387–394

Righter K, Drake MJ (1999) Effect of water on metal-silicate partitioning of siderophile elements'' a high pressure and temperature terrestrial magma ocean and core formation. Earth Planet Sci Lett 171:383–399

Roberts JJ, Tyburczy JA (1991) Frequency dependent electrical properties of polycrystalline olivine compacts. J Geophys Res 96(B10):16205–16222

Roberts JJ, Tyburczy JA (1993) Impedance spectroscopy of single and polycrystalline olivine: evidence for grain boundary transport. Phys Chem Miner 20:19–26

Roberts JJ, Tyburczy JA (1994) Frequency-dependent electrical properties of minerals and partial-melts. Surv Geophys 15:239–262

Roberts JJ, Tyburczy JA (1999) Partial-melt electrical conductivity: influence of melt composition. J Geophys Res 104:7055–7065

Roberts JJ, Tyburczy JA (2000) Partial-melt conductivity: influence of melt composition. J Geophys Res 104:7055–7065

Rohrbach A, Schmidt MW (2011) Redox freezing and melting in the Earth's deep mantle resulting from carbon–iron redox coupling. Nature. doi:10.1038/nature09899

Roling B (1999) What do electrical conductivity and electrical modulus spectra tell us about the mechanisms of ion transport processes in melts, glasses, and crystals? J Non Cryst Solids 244:34–43

Romano C, Poe BT, Tyburczy J, Nestola F (2009) Electrical conductivity of hydrous wadsleyite. Eur J Mineral 21:615–622

Saal AE, Hauri EH, Langmuir CH, Perfit MR (2002) Vapour undersaturation in primitive mid-ocean-ridge basalt and the volatile content of earth's upper mantle. Nature 419:451–455

Satherley J, Smedley SI (1985) The electrical conductivity of some hydrous and anhydrous molten silicates as a function of temperature and pressure. Geochim Cosmochim Acta 49:769–777

Sato H (1986) High temperature a.c. electrical properties of olivine single crystal with varying oxygen partial pressure: implications for the point defect chemistry. Phys Earth Planet Int 41:269–282

Sato H, Ida Y (1984) Low frequency electrical impedance of partially molten gabbro: the effect of melt geometry on electrical properties. Tectonophysics 107:105–134

Schmidt MW, Poli S (1998) Experimentally based water budgets for dehydrating slabs and consequences for arc magma generation. Earth Planet Sci Lett 163:361–379

Schock RN, Duba AG, Shankland TJ (1989) Electrical conduction in olivine. J Geophys Res 94:5829–5839

Schultz A (1990) On the vertical gradient and associated heterogeneity in mantle electrical conductivity. Phys Earth Planet Int 64:68–86

Seaman C, Sherman SB, Garcia MO, Baker MB, Balta B, Stolper E (2004) Volatiles in glasses from the HSDP2 drill core. Geochem Geophys Geosyst. doi:10.1029/2003GC000596

Shankland TJ, Waff HS (1977) Partial melting and electrical conductivity anomalies in the upper mantle. J Geophys Res 82:5409–5417

Shankland TJ, Peyronneau J, Poirier J-P (1993) Electrical conductivity of the earth's lower mantle. Nature 366:453–455

Shankland TJ, Duba AG, Mathez EA, Peach CL (1997) Increase of electrical conductivity with pressure as an indicator of conduction through a solid phase in midcrustal rocks. J Geophys Res 102(B7):14741–14750

Shaw HR (1965) Comments on viscosity, crystal settling, and convection in granitic magmas. Am J Sci 263:120–152

Shimojuku A, Yoshino T, Yamazaki D, Okudaira T (2012) Electrical conductivity of fluid-bearing quartzite under lower crustal conditions. Phys Earth Planet Int 198–199:1–8

Simonnet C, Phalippou J, Malki M (2003) Electrical conductivity measurements of oxides from molten state to glassy state. Rev Sci Inst 74:2805–2810

Simpson F (2002) Intensity and direction of lattice-preferred orientation of olivine: are electrical and seismic anisotropies of the Australian mantle reconcilable? Earth Planet Sci Lett 203:535–547

Simpson F, Bahr R (2005) Practical magnetotellurics. Cambridge University Press, Cambridge, 270 pp. doi:10.1017/CBO9780511614095

Simpson F, Tommassi A (2005) Hydrogen diffusivity and electrical anisotropy of a peridotite sample. Geophys J Int 160:1092–1102

Simpson F, Warner M (1998) Coincident magnetotelluric, P-wave and S-wave images of the deep continental crust beneath the Weardale granite, NE England: seismic layering, low conductance and implications against the fluids paradigm. Geophys J Int 133:419–434

Skrotzy W (1994) Defect structure and deformation mechanisms in naturally deformed augite and enstatite. Tectonophysics 229:43–68

Smyth JR (1987) A crystallographic model for hydrous wadsleyite(β-Mg$_2$SiO$_4$): an ocean in the earth's interior? Am Mineral 79:1021–1024

Smyth JR, Holl CM, Frost DJ, Jacobsen SD, Langenhorst F, McCammon CA (2003) Structural systematics of hydrous ringwoodite and water in earth's interior. Am Mineral 88(10):1402–1407

Song TRA, Helmberger DV, Grand SP (2004) Low-velocity zone atop the 410-km seismic discontinuity in the northwestern United States. Nature 427:530–533

Stachel T, Brey GP, Harris JW (2005) Inclusions in sublithospheric diamonds: glimpses of deep Earth. Elements 1:73–78

Stesky RM (1986) Electrical conductivity of brine-saturated fractured rock. Geophysics 51(8):1585–1593

Stesky RM, Brace WF (1973) Electrical conductivity of serpentinized rocks to 6 kilobars. J Geophys Res 78:7614–7621

Takei Y (2000) Acoustic properties of partially molten media studied on a simple binary system with a controllable dihedral angle. J Geophys Res 105(B7):16665–16682

Tarits P, Hautot S, Perrier F (2004) Water in the mantle: results from electrical conductivity beneath the French Alps. Geophys Res Lett 31:L06612. doi:10.1029/2003GL019277

ten Grotenhuis SM, Drury MR, Spiers CJ, Peach CJ (2005) Melt distribution in olivine rocks based on electrical conductivity measurement. J Geophys Res 110:B12201. doi:10.1029/2004JB003462

Tenner TJ, Hirschmann MM, Withers AC, Hervig RL (2009) Hydrogen partitioning between nominally anhydrous upper mantle minerals and melt between 3 and 5 GPa and applications to hydrous peridotite partial melting. Chem Geol 262:42–56

Tenner TJ, Hirschmann MM, Withers AC, Ardia P (2012) H$_2$O storage capacity of olivine and low-Ca pyroxene from 10 to 13 GPa: consequences for dehydration melting above the transition zone. Contrib Mineral Petrol 163:297–316

Toffelmier DA, Tyburczy JA (2007) Electromagnetic detection of a 410-km-deep melt layer in the southwestern United States. Nature 447. doi:10.1038/nature05922

Tolland HG (1973) Mantle conductivity and electrical properties of garnet, mica and amphibole. Nat Phys Sci 241:35–36

Tyburczy JA (2007) Properties of rocks and minerals—the electrical conductivity of rocks, minerals and the earth. Treatise Geophys 2:631–642

Tyburczy JA, Fisler DK (1995) Electrical properties of minerals and melts. Mineral physics and crystallography: a handbook of physical constants. AGU Reference Shelf 2 185–208

Tyburczy JA, Waff HS (1983) Electrical conductivity of molten basalt and andesite to 25 kilobars pressure: geophysical significance and implications for charge transport and melt structure. J Geophys Res 88(B3):2413–2430

Utada H, Koyama T, Shimizu H (2003) A semi-global reference model for electrical conductivity in the mid-mantle beneath the north Pacific region. Geophys Res Lett 31:1194. doi:10.1029/2002GL016902

Utada H, Koyama T, Obayashi M, Fukao Y (2009) A joint interpretation of electromagnetic and seismic tomography models suggests the mantle transition zone below Europe is dry. Earth Planet Sci Lett 281:249–257

Verhoeven O, Mocquet A, Vacher P, Rivoldini A, Menvielle M, Arrial P-A, Choblet G, Tarits P, Dehant V, Van Hoolst T (2009) Constraints on thermal state and composition of the earth's lower mantle from electromagnetic impedances and seismic data. J Geophys Res 114:B03302. doi:10.1029/2008JB005678

Vetere F, Behrens H, Holtz F, Vilardo G, Ventura G (2010) Viscosity of crystal-bearing melts and its implication for magma ascent. J Mineral Petrol Sci 105:151–163

Volarovich MP, Tolstoi DM (1936) The simultaneous measurement of viscosity and electrical conductivity of some fused silicates at temperatures up to 1400°C. J Soc Glass Technol 20:54–60

Volarovich MP, Bondarenko AT, Parkhomenko EI (1962) The influence of pressure on the electrical properties of rocks. Proc Inst Phys Earth Mosc 23:80–90

von Bargen N, Waff HS (1986) Permeabilities, interfacial areas and curvatures of partially molten systems: results of numerical computations of equilibrium microstructures. J Geophys Res 91:9261–9276

Waff HS (1974) Theoretical considerations of electrical conductivity in a partially molten mantle and implications for geothermometry. J Geophys Res 79:4003–4010

Waff HS, Weill DF (1975) Electrical conductivity of magmatic liquids: effects of temperature, oxygen fugacity and composition. Earth Planet Sci Lett 28:254–260

Wang D, Mookherjee M, Xu YS, Karato S (2006) The effect of hydrogen on the electrical conductivity in olivine. Nature 443:977–980

Wang D, Li H, Yi L, Matsuzaki T, Yoshino T (2010) Anisotropy of synthetic quartz electrical conductivity at high pressure and temperature. J Geophys Res 115:B09211. doi:10.1029/2009JB006695

Wang D, Guo Y, Yu Y, Karato S-I (2012) Electrical conductivity of amphibole-bearing rocks: influence of dehydration. Contrib Mineral Petrol. doi:10.1007/s00410-012-0722-z

Wannamaker PE (2005) Anisotropy versus heterogeneity in continental solid earth electromagnetic studies: fundamental response characteristics and implications for physiochemical state. Surv Geophys 26:733–765

Wannamaker PE, Caldwell TG, Jiracek GR, Maris V, Hill GJ, Ogawa Y, Bibby HM, Bennie SL, Heise W (2009) Fluid and deformation regime of an advancing subduction system at Marlborough, New Zealand. Nature 460:733–736

Watanabe T, Kurita K (1993) The relationship between electrical conductivity and melt fraction in a partially molten simple system. Phys Earth Planet Int 78:9–17

Watson EB, Brennan JM (1987) Fluids in the lithosphere, 1. Experimentally-determined wetting characteristics of CO2-H2O fluids and their implications for fluid transport, host-rock physical properties, and fluid inclusion formation. Earth Planet Sci Lett 85:497–515

Watson HC, Roberts JJ, Tyburczy JA (2010) The effect of conductive grain boundary impurities on electrical conductivity in polycrystalline olivine. Geophys Res Lett 37:L02303. doi:10.1029/2009GL041566

Weidelt P (1999) 3D conductivity models: implications of electrical anisotropy. In: Oristaglio M, Spies B (eds) Three-dimensional electromagnetics. Society of Exploration Geophysicists, Tulsa, pp 119–137

Wendlandt RF, Huebner JS, Harrison WL (1982) The redox potential of boron nitride and implications for its use as a crucible material in experimental petrology. Am Mineral 67:170–174

Williams Q, Hemley RJ (2001) Hydrogen in the deep earth. Annu Rev Earth Planet Sci 29:365–418

Withers AC, Bureau H, Raepsaet C, Hirschmann MM (2012) Calibration of infrared spectroscopy by elastic recoil detection analysis of H in synthetic olivine. Chem Geol 334:92–98

Worzewski T, Jegen M, Kopp H, Brasse H, Castillo WT (2011) Magnetotelluric image of the fluid cycle in the Costa Rican subduction zone. Nat Geosci 4:108–111. doi:10.1038/NGEO1041

Wunder B (1998) Equilibrium experiments in the system MgO-SiO2-H2O(MSH): stability fields of clinohumite-OH [Mg9Si4O16 (OH)2], chondrodite-OH [Mg5Si2O8(OH)2] and phase A [Mg7Si2O8(OH)6]. Contrib Mineral Petrol 132:111–120

Wyllie PJ, Baker MB, White BS (1990) Experimental boundaries for the origin and evolution of carbonatites. Lithos 26:3–19

Xu Y, Poe BT, Shankland TJ, Rubie DC (1998) Electrical conductivity of minerals of the mantle transition zone. Science 280:1415–1418

Xu Y, Shankland TJ, Duba A (2000) Pressure effect on electrical conductivity of mantle olivine. Phys Earth Planet Int 118:149–161

Yagi T, Akaogi M, Shimomura O, Suzuki T, Akimoto S (1987) In situ observation of the olivine-spinel phase transformation in Fe_2SiO_4 using synchrotron radiation. J Geophys Res 92:6207–6213

Yang X (2011) Origin of high electrical conductivity in the lower continental crust: a review. Surv Geophys 32:875–903

Yang X (2012) Orientation-related electrical conductivity of hydrous olivine, clinopyroxene and plagioclase and implications for the structure of the lower continental crust and uppermost mantle. Earth Planet Sci Lett 317–318:241–250

Yang X, Heidelbach F (2012) Grain size effect on the electrical conductivity of clinopyroxene. Contrib Mineral Petrol 163:939–947

Yang X, McCammon C (2012) Fe^{3+}-rich augite and high electrical conductivity in the deep. Geology 40(2):131–134. doi:10.1130/G32725

Yang X, Keppler H, McCammon C, Ni H, Xia Q, Fan Q (2011) The effect of water on the electrical conductivity of lower crustal clinopyroxene. J Geophys Res 116:B04208. doi:10.1029/2010JB008010

Yang X, Keppler H, McCammon C, Ni H (2012) Electrical conductivity of orthopyroxene and plagioclase in the lower crust. Contrib Mineral Petrol 163:33–48. doi:10.1007/s00410-011-0657-9

Yoshino T (2010) Laboratory electrical conductivity measurement of mantle minerals. Surv Geophys 31:163–206. doi:10.1007/s10712-009-9084-0

Yoshino T, Katsura T (2009) Effect of iron content on electrical conductivity of ringwoodite, with implications for electrical structure in the mantle transition zone. Phys Earth Planet Int 174:3–9

Yoshino T, Katsura T (2012) Re-evaluation of electrical conductivity of anhydrous and hydrous wadsleyite. Earth Planet Sci Lett 337–338:56–67

Yoshino T, Takuya M, Yamashita S, Katsura T (2006) Hydrous olivine unable to account for conductivity anomaly at the top of the asthenosphere. Nature 443:973–976

Yoshino T, Manthilake G, Matsuzaki T, Katsura T (2008) Dry mantle transition zone inferred from the conductivity of wadsleyite and ringwoodite. Nature 451:326–329

Yoshino T, Yamazaki D, Mibe K (2009) Well-wetted olivine grain boundaries in partial molten peridotites in the asthenosphere. Earth Planet Sci Lett 283:167–173

Yoshino T, Laumonier M, McIsaac E, Katsura T (2010) Electrical conductivity of basaltic and carbonatite melt-bearing peridotites at high pressures: Implications for melt distribution and melt fraction in the upper mantle. Earth Planet Sci Lett 295:593–602

Yoshino T, Ito E, Katsura T, Yamazaki D, Shan S, Guo X, Nishi M, Higo Y, Funakoshi K-i (2011) Effect of iron content on electrical conductivity of ferropericlase with implications for the spin transition pressure. J Geophys Res 116:B04202. doi:10.1029/2010JB007801

Yoshino T, McIsaac E, Laumonier M, Katsura T (2012) Electrical conductivity of partial molten carbonate peridotite. Phys Earth Planet Int 194–195:1–9

Zhang G-H, Chou K-C (2010) Simple method for estimating the electrical conductivity of oxide melts with optical basicity. Metall Trans B 41B:131–136

Zhang S, Karato S-I (1995) Lattice preferred orientation of olivine aggregates deformed in simple shear. Nature 375:774–777

Zhang B, Yoshino T, Wu X, Matsuzaki T, Shan S, Katsura T (2012) Electrical conductivity of enstatite as a function of water content: implications for the electrical structure in the upper mantle.Earth Planet Sci Lett 357–358, 11–20

Zhu M, Xie H, Guo J, Xu Z (2001) An experimental study of the conductivity of talc at high temperature and high pressure. Chin J Geophys 44:429–435

Zimmerman GH, Gruszkiewicz MS, Wood RH (1995) New apparatus for conductance measurements at high temperatures: conductance of aqueous solutions of LiCl, NaCl, NaBr, and CsBr at 28 MPa and water densities from 700 to 260 kg m^{-3}. J Phys Chem 99:11612–11625

Zimmerman ME, Zhang S, Kohlstedt DL, Karato S-i (1999) Melt distribution in mantle rocks deformed in shear. Geophys Res Lett 26:1505–1508

Zimmerman GH, Scott PW, Greynolds W (2007) A new flow instrument for conductance measurements at elevated temperatures and pressures: measurements on NaCl(aq) to 458 K and 1.4 MPa. J Solution Chem 36:767–786